What can we learn from neutron monitor multiplicities?

Alejandro Sáiz
Mahidol University

When an energetic cosmic ray comes to Earth …

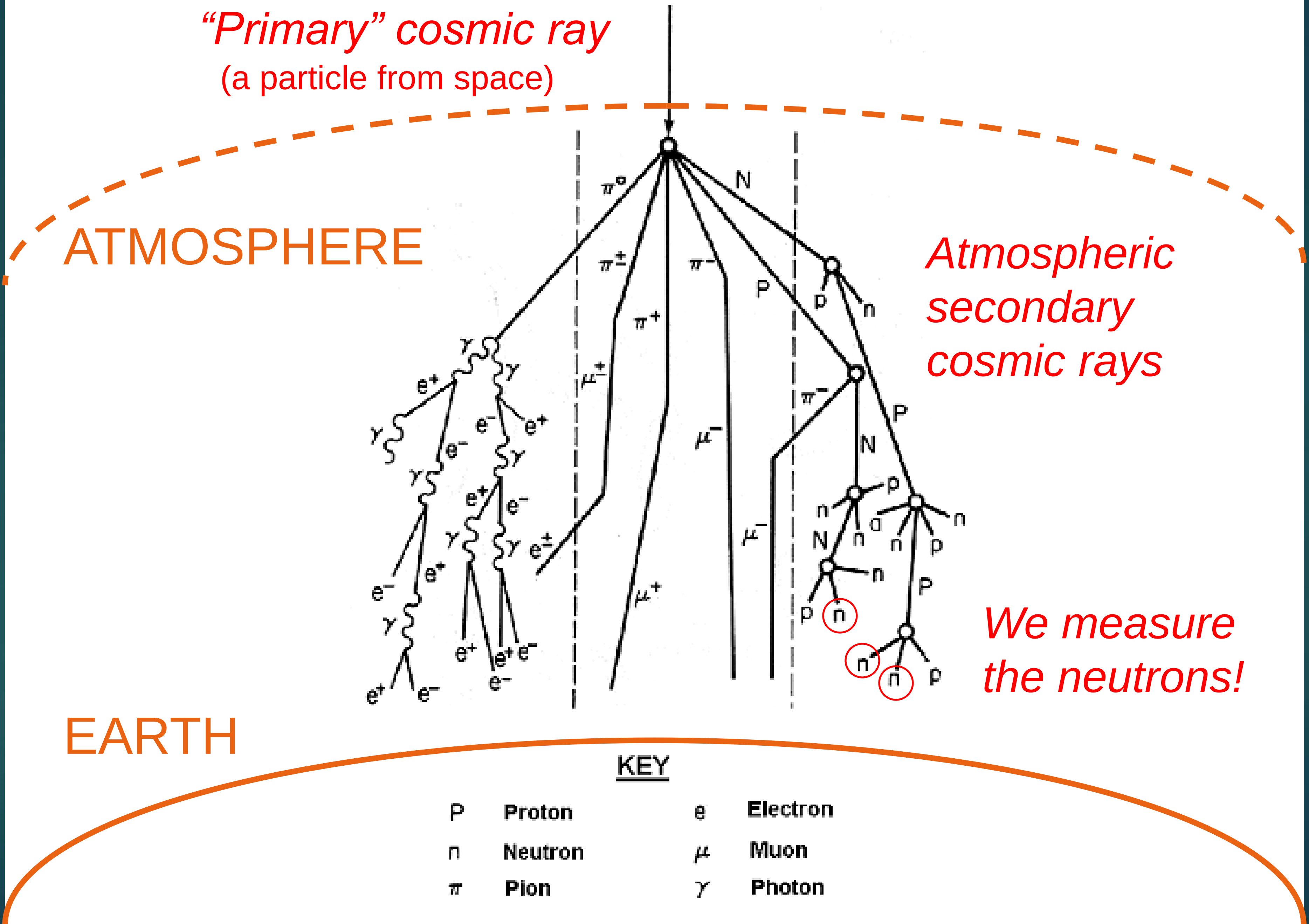

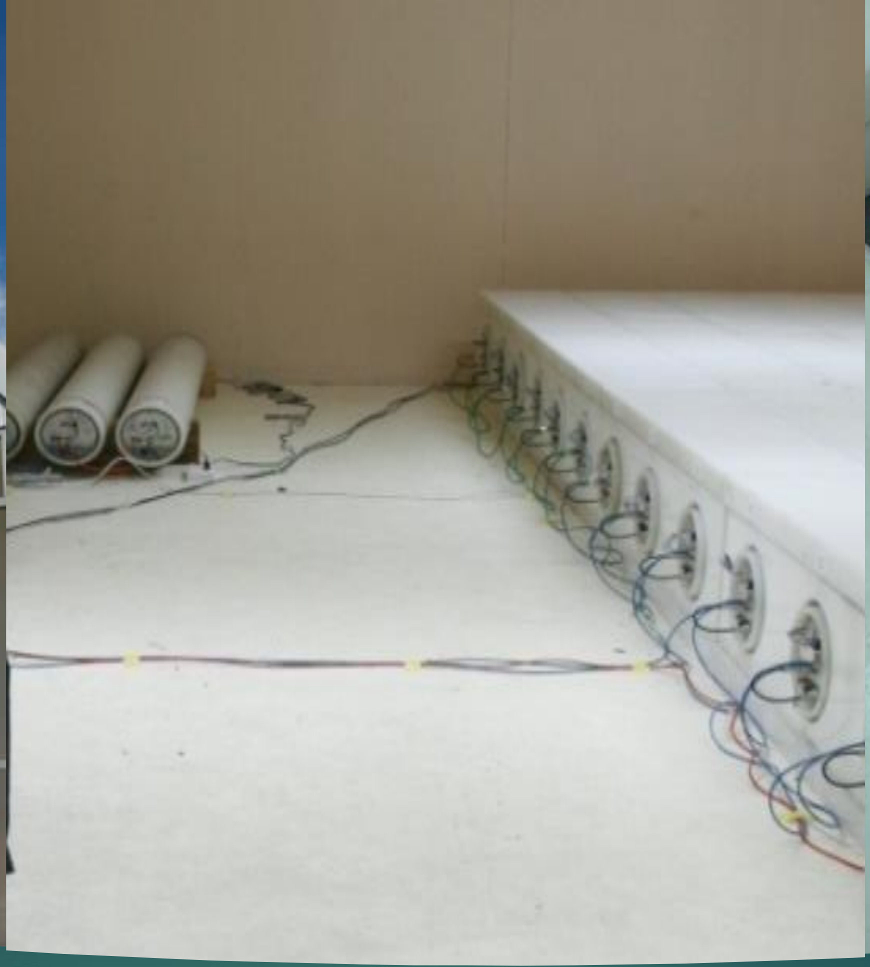
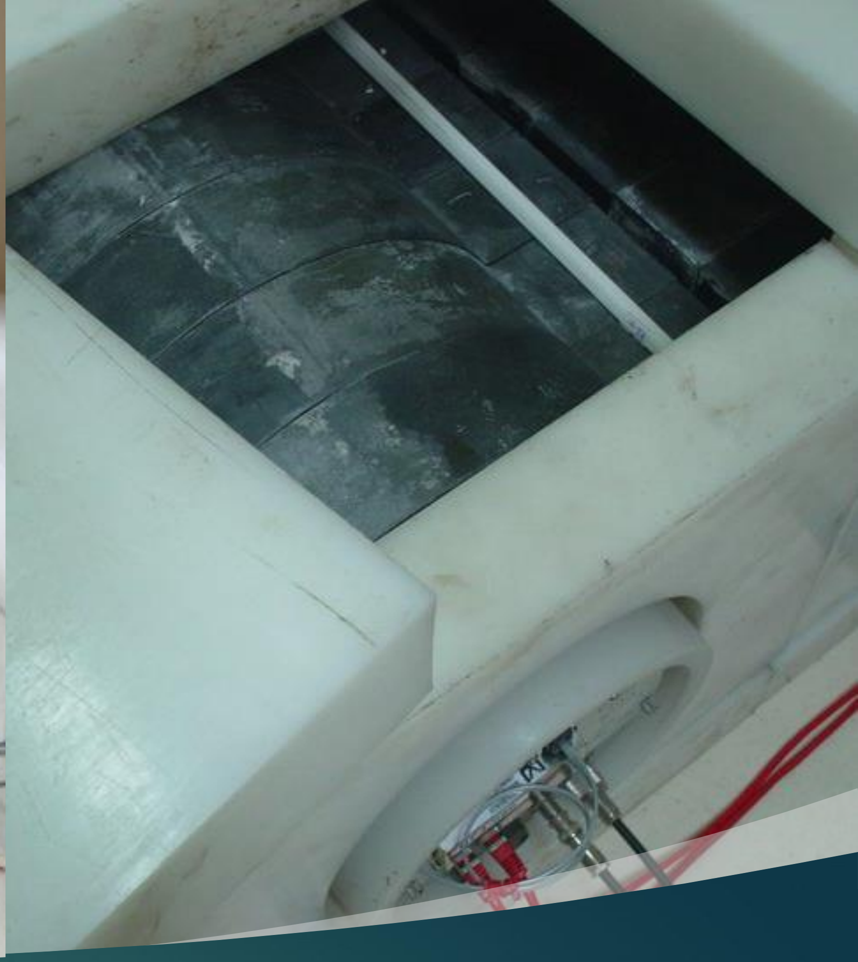

Princess Sirindhorn Neutron Monitor

Neutron Detectors

Neutron Monitors

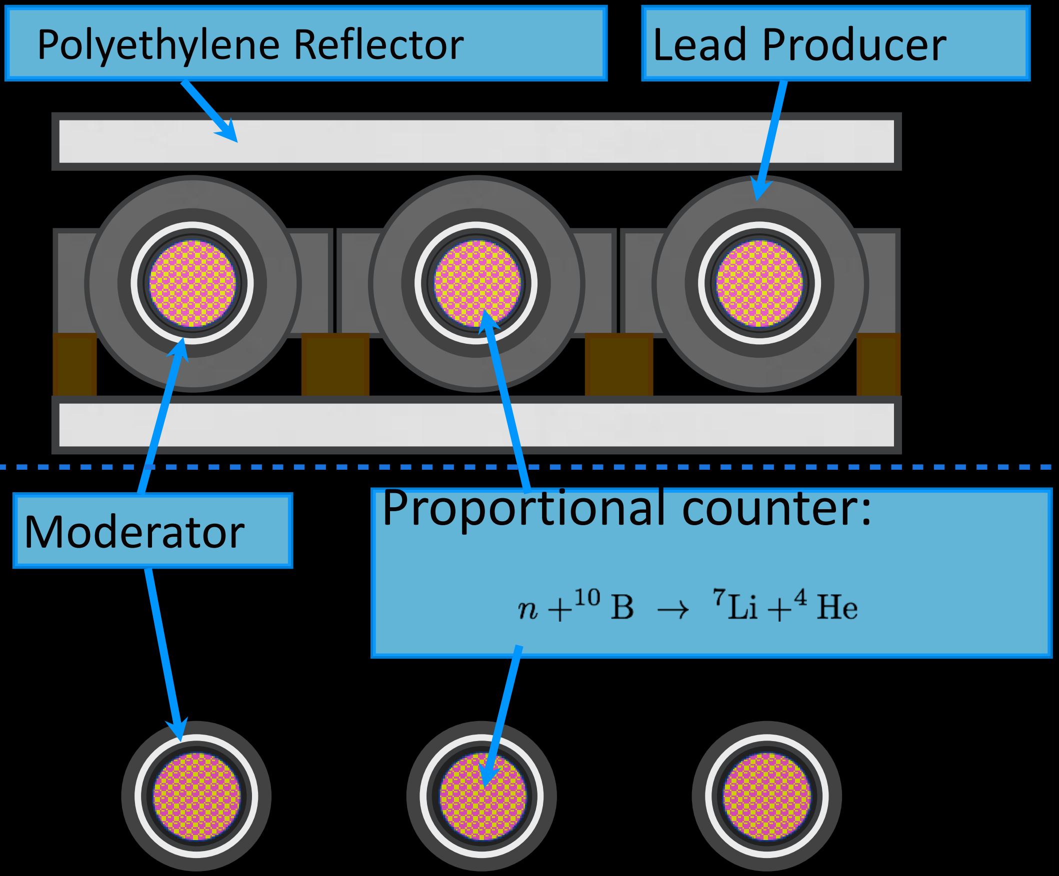

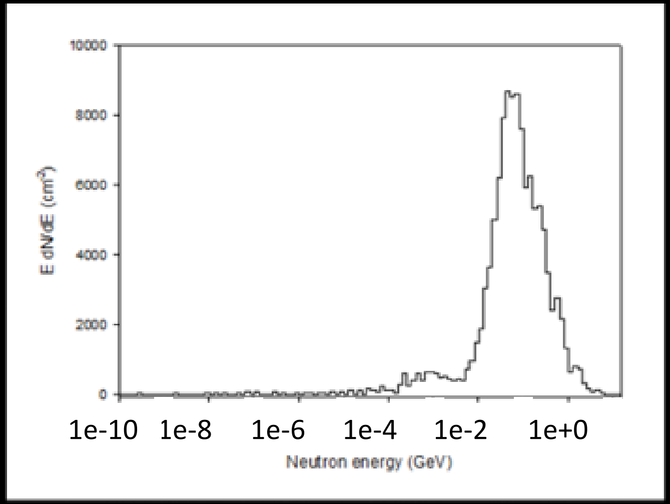

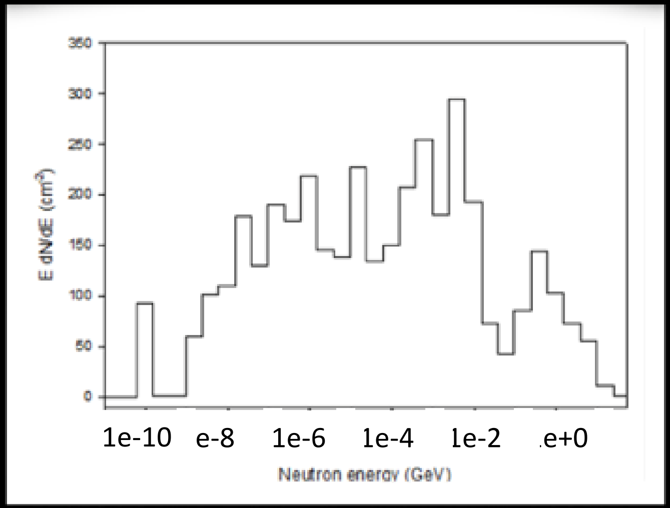

Bare Neutron Detectors

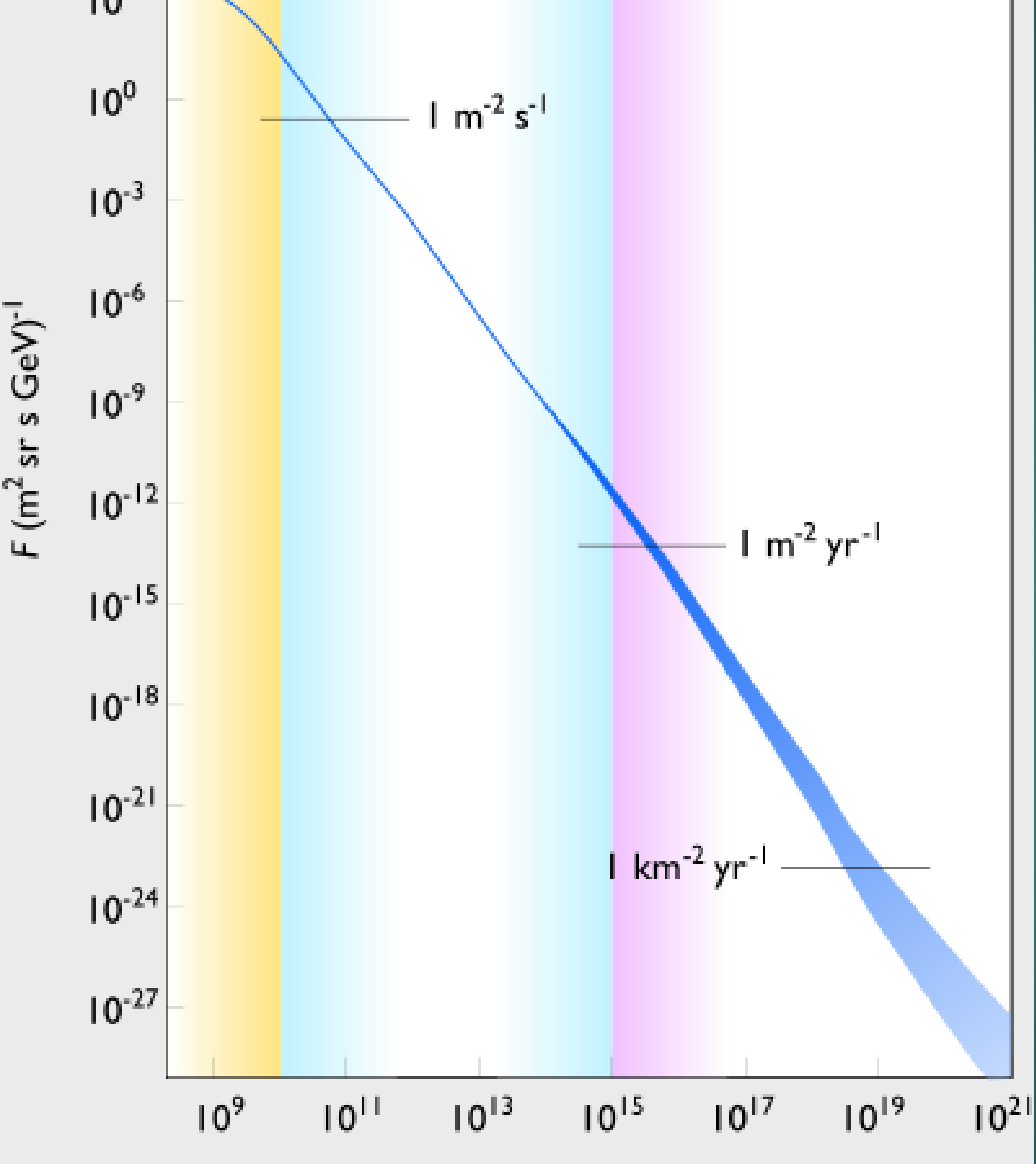

Spectrum of Primary Cosmic Rays (Outside Earth's Atmosphere)

- Steep decrease with energy (power law)
- Image: Wikipedia

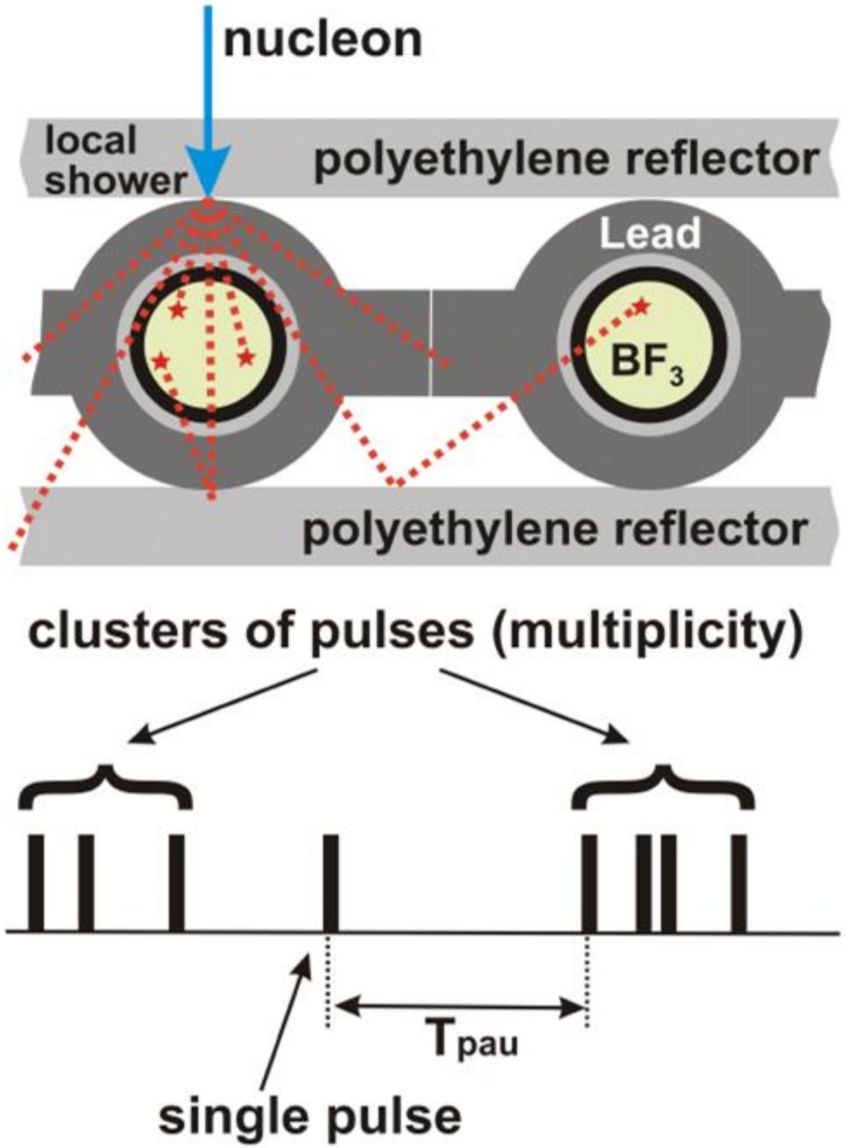

Multiplicity and cosmic ray energy

- *NMs were originally designed to give a count rate as a proxy of cosmic ray flux through Earth's magnetic field at a location*
- *No energy information*
- *The producer (Pb) is used to amplify the signal: multiple counts per event*
- *Multiplicity increases with energy*

[Yu. V. Balabin et al, 2011]

Same-counter analysis

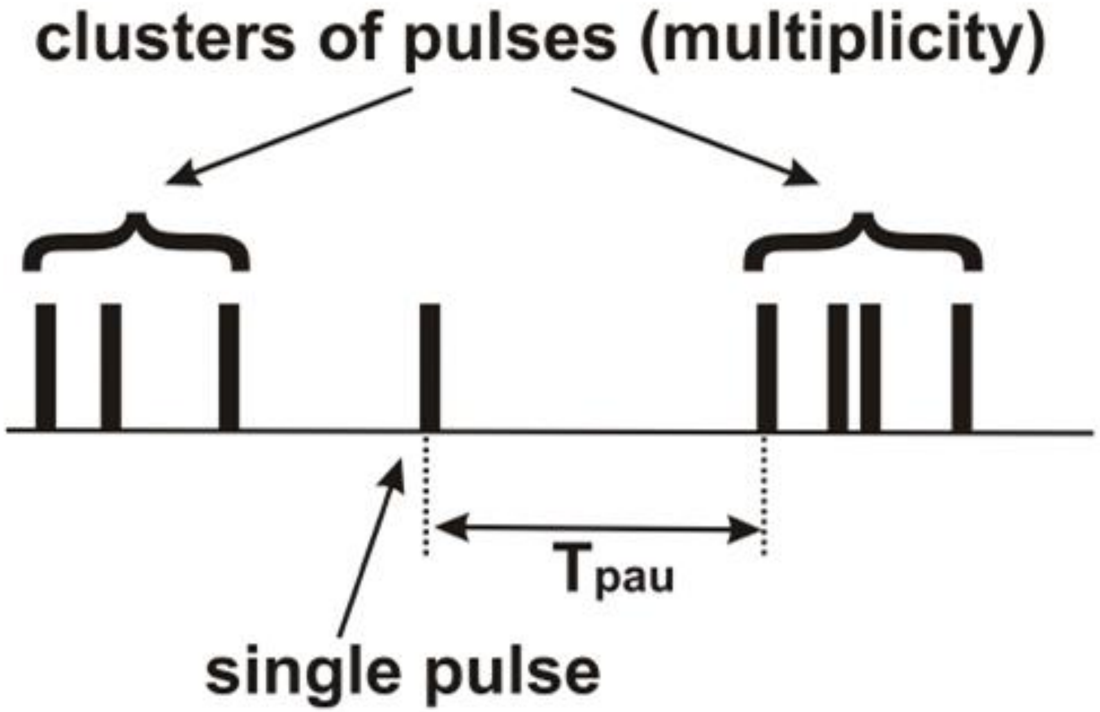

- *Data needed: times of detection, or between detections (pulses)*
- *Time between clusters of pulses on average much longer than time within pulses in a cluster…*
- *…but can be shorter! (→ chance coincidence)*
- *Electronics have a dead time*

[Yu. V. Balabin et al, 2011]

Window multiplicity

- *Suggested by Hughes et al (1964)*
- *Implemented as hardware: "multiplicity analyzer"*
- *Nowadays implemented in software*
- *Multiplicity inside a "time window"*

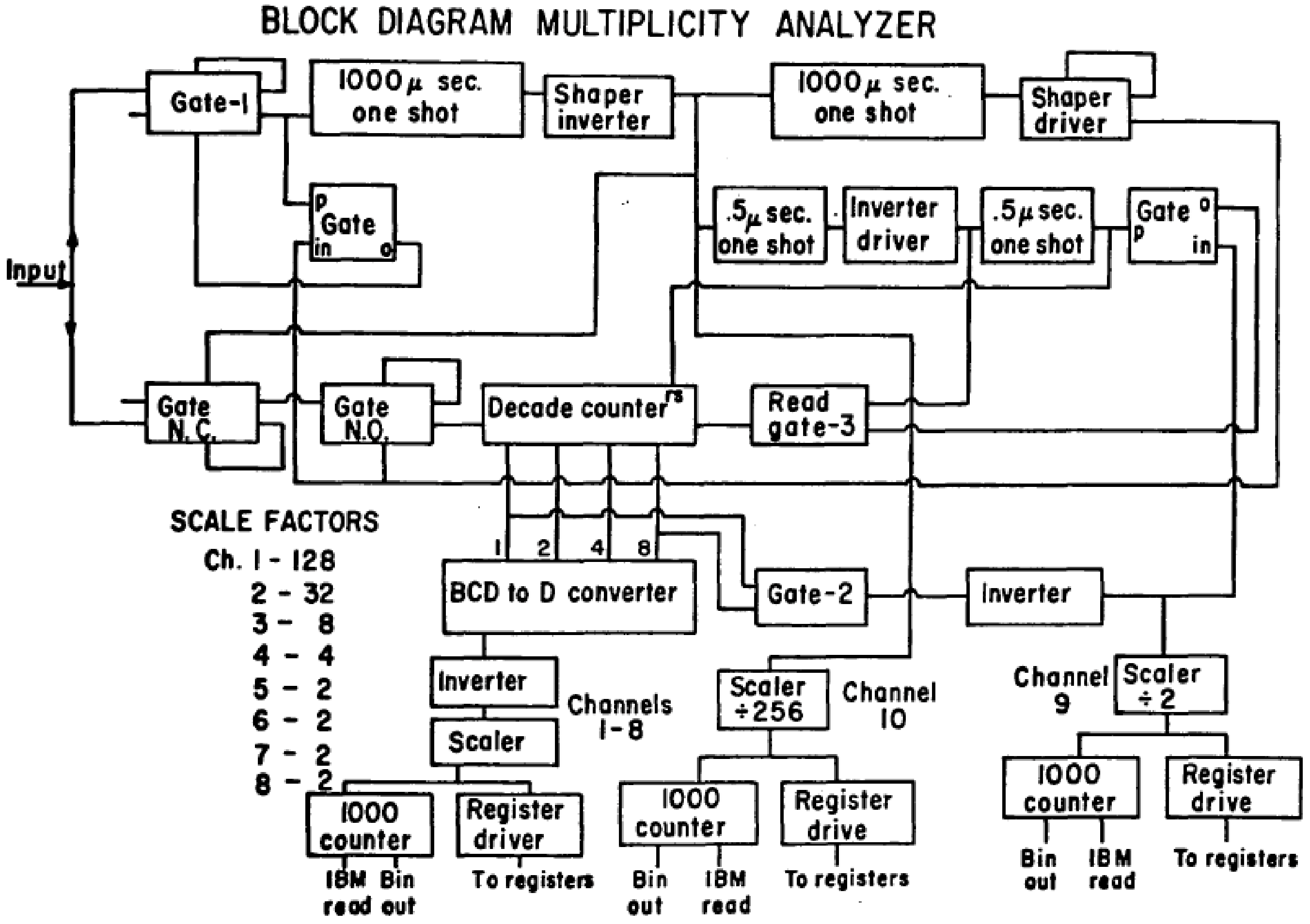

[P. Singh PhD thesis, 1971]

Window multiplicity

- *Multiplicity rates R_1, R_2, …, R_n record number of events with n detections within the window*
- *Cross contamination due to chance coincidences not simple to remove*

$$R_1 = R_1' D$$

$$R_2 = \frac{R_2' D - R_1^2 \, T_g \, \bar{W}_1^1}{1 + R_1 \, T_g \, \bar{W}_1^2}$$

$$R_3 = \frac{R_3' D - [R_2 R_1 T_g \bar{W}_1^1 + R_2^2 T_g \bar{W}_1^2 + 1/2 R_1^3 (T_g \bar{W}_1^1)^2 + R_1 R_2 T_g \bar{W}_2^2]}{1 + R_1 T_g \bar{W}_2^3}$$

$$R_4 = \frac{R_4' D - \left[\begin{array}{l} R_3 R_1 T_g \bar{W}_1^1 + R_3 R_2 T_g \bar{W}_1^2 + 1/2 R_2 (R_1 T_g \bar{W}_1^1)^2 \\ + R_2^2 T_g \bar{W}_2^2 + R_2 R_3 T_g \bar{W}_2^3 + R_2 (R_1 T_g)^2 \bar{W}_1^1 \bar{W}_2^2 + R_1 R_3 T_g \bar{W}_3^3 \end{array}\right]}{1 + R_1 T_g \bar{W}_3^4}$$

$$R_k = \frac{R_k' D - [\sum_{i=1}^{k-1} R_i \, R_{k-i} \, T_g \, \bar{W}_i^i]}{1 + R_1 T_g \bar{W}_{k-1}^k} , \quad 5 \le k \le 8$$

$$R_{\geq 9} = R_{\geq 9}'$$

[P. Singh PhD thesis, 1971]

Use of two dead times: Apatity NM

*"The **dead time** is the period during which the registration channel is closed after detecting the next neutron. There are two kinds of Apatity NM count rate data: with **Large dead time** (LDT) and **Small dead time** (SDT). The size of LDT, 1200 microseconds, is chosen so that to block the channel on a lifetime of multiplicity neutrons in the neutron monitor. Thus, at use the LDT to each primary neutron there corresponds one pulse. The result is in a better statistical accuracy of registered count rate of neutrons. Compensation of losses because of dead time is provided with a special electronic circuit. The channel with SDT, 10 microseconds (same as in the original neutron monitor of Charmichael), collects pulses from all registered neutrons, including ones of multiplicity."*

http://pgia.ru/cosmicray/

Use of two dead times: Apatity NM

LDT count rate is the rate of clusters of pulses

Comparing LDT with SDT rates, multiplicity can be obtained

Chance coincidences are difficult to deal with, rate of clusters may be understimated

Time-delay distributions

- Distribution of times between consecutive detections shows an exponential tail of uncorrelated counts
- Bieber et al. (2004) used Monte Carlo simulations to reproduce observed histograms for a given CR spectrum, but discrepancies were significant

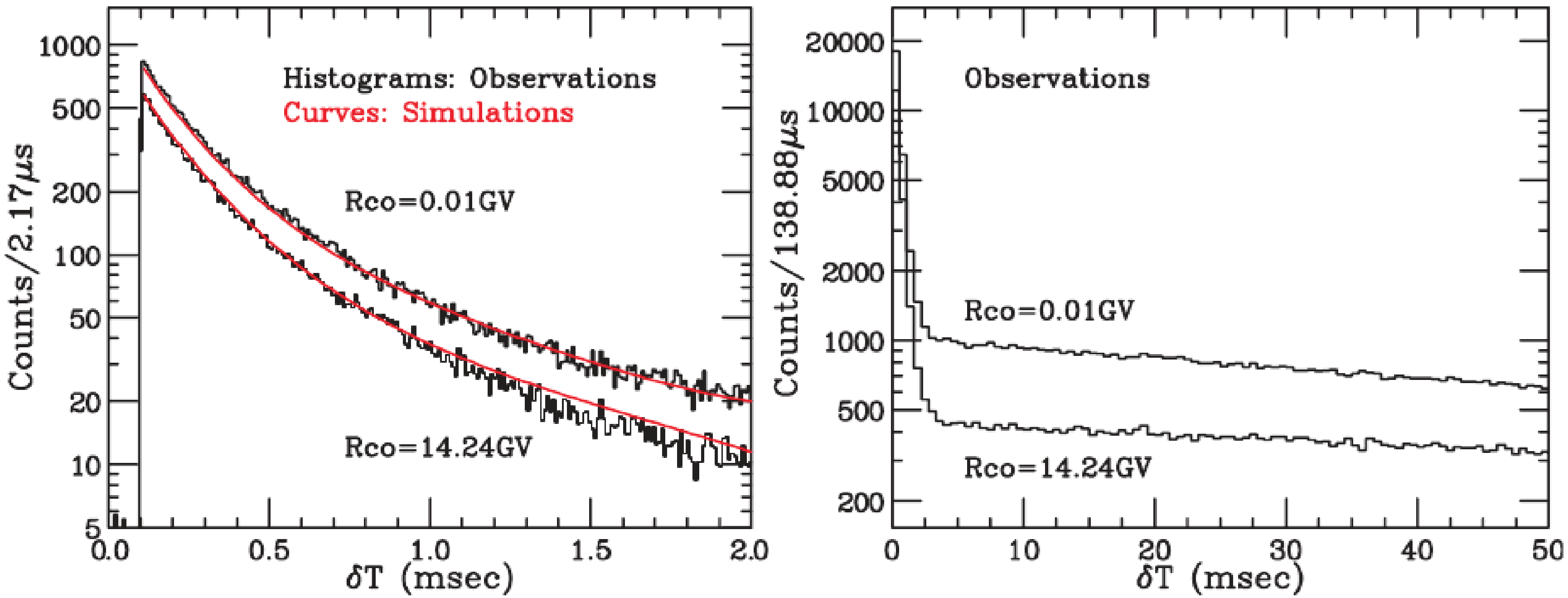

[J. W. Bieber et al, 2004]

Time-delay distributions

- Ruffolo et al (2016) used an exponential fit to estimate the rate of clusters (or "leaders")
- Chance coincidences do not affect the result
- The ratio of leader pulses to total pulses, or "leader fraction", can be interpreted as inverse multiplicity

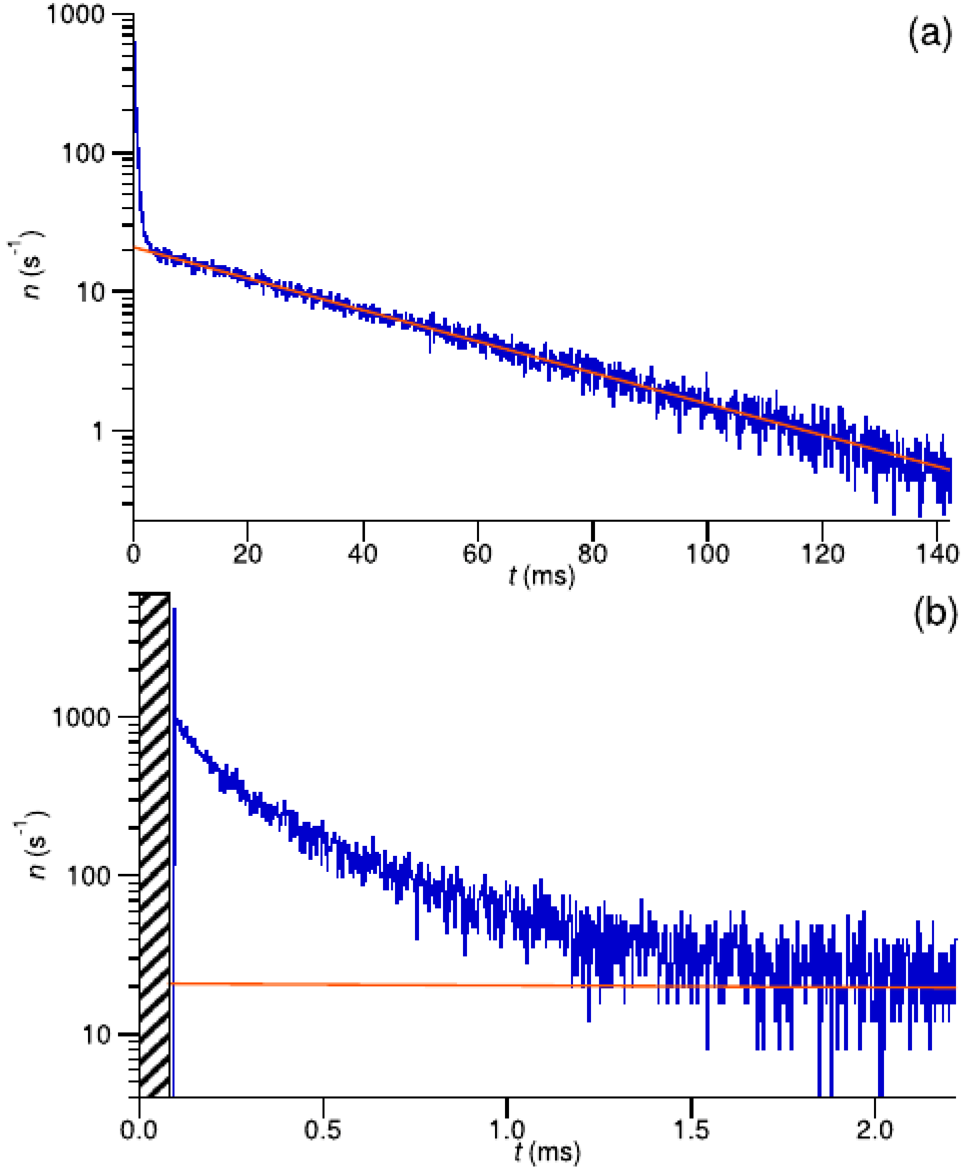

[D. Ruffolo et al, 2016]

Leader fraction

- *Mangeard et al (2016) showed how the leader fraction depended on the geomagnetic cutoff and on solar modulation during a series of latitude surveys*

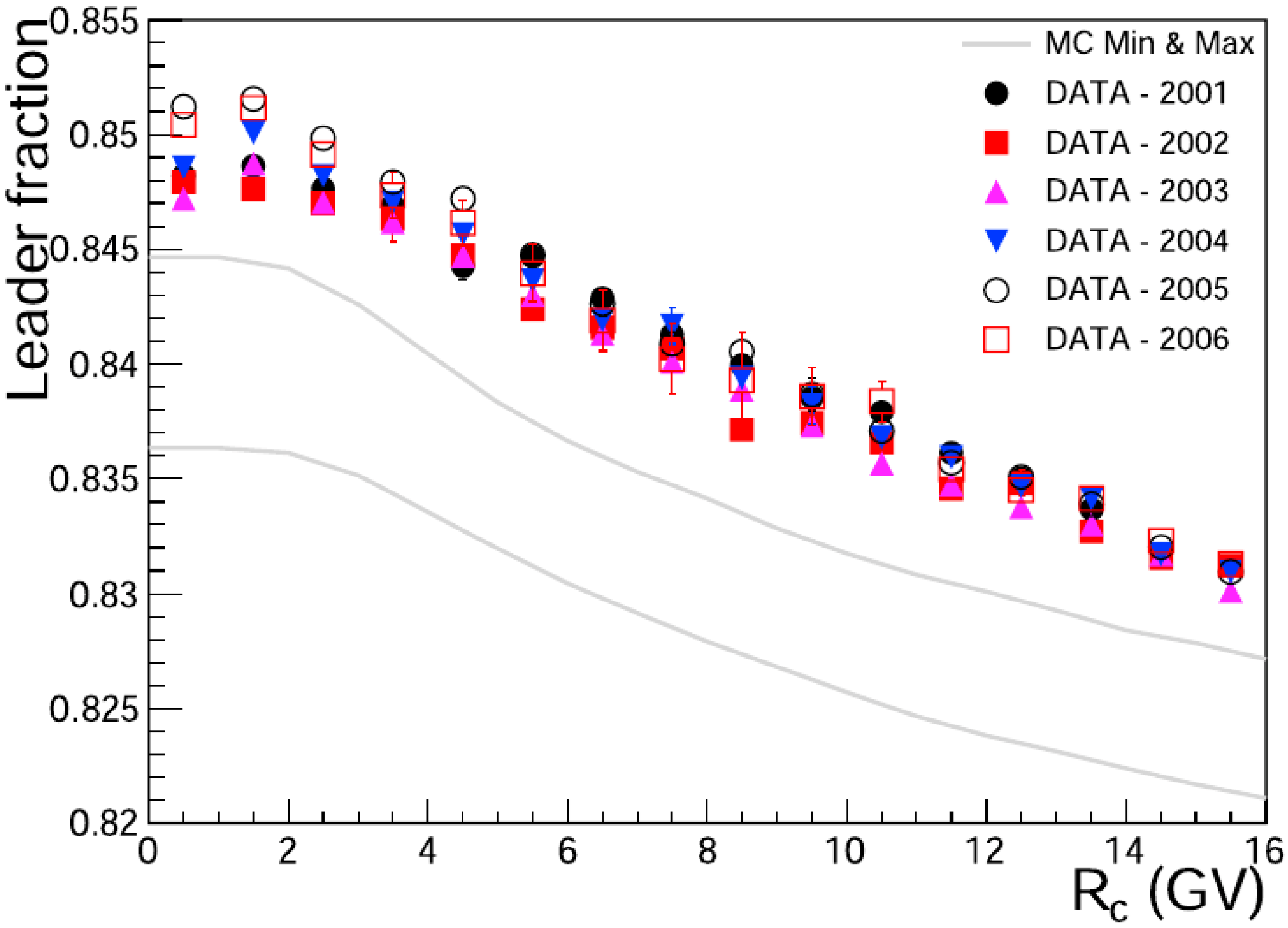

[P.-S. Mangeard et al, 2016]

Leader fraction

- *Banglieng et al (2020) presented a 10-year long time series of leader fraction L at the Princess Sirindhorn Neutron Monitor at high rigidity cutoff, showing variations of interest*

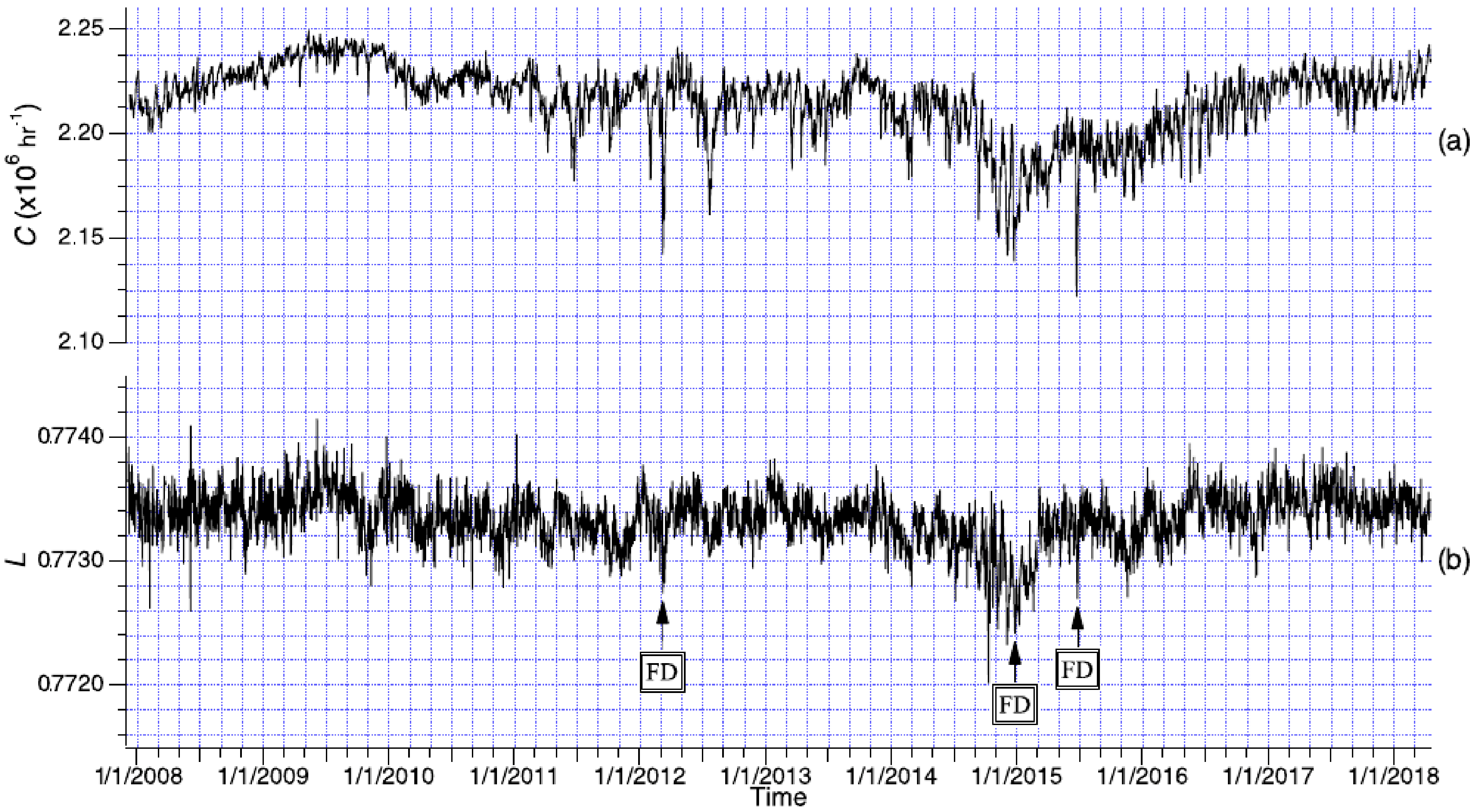

[C. Banglieng et al, 2020]

Leader fraction

- *Banglieng et al (2020) presented a 3-year long time series of leader fraction L at the South Pole Neutron Monitor at high rigidity cutoff, showing variations of interest*

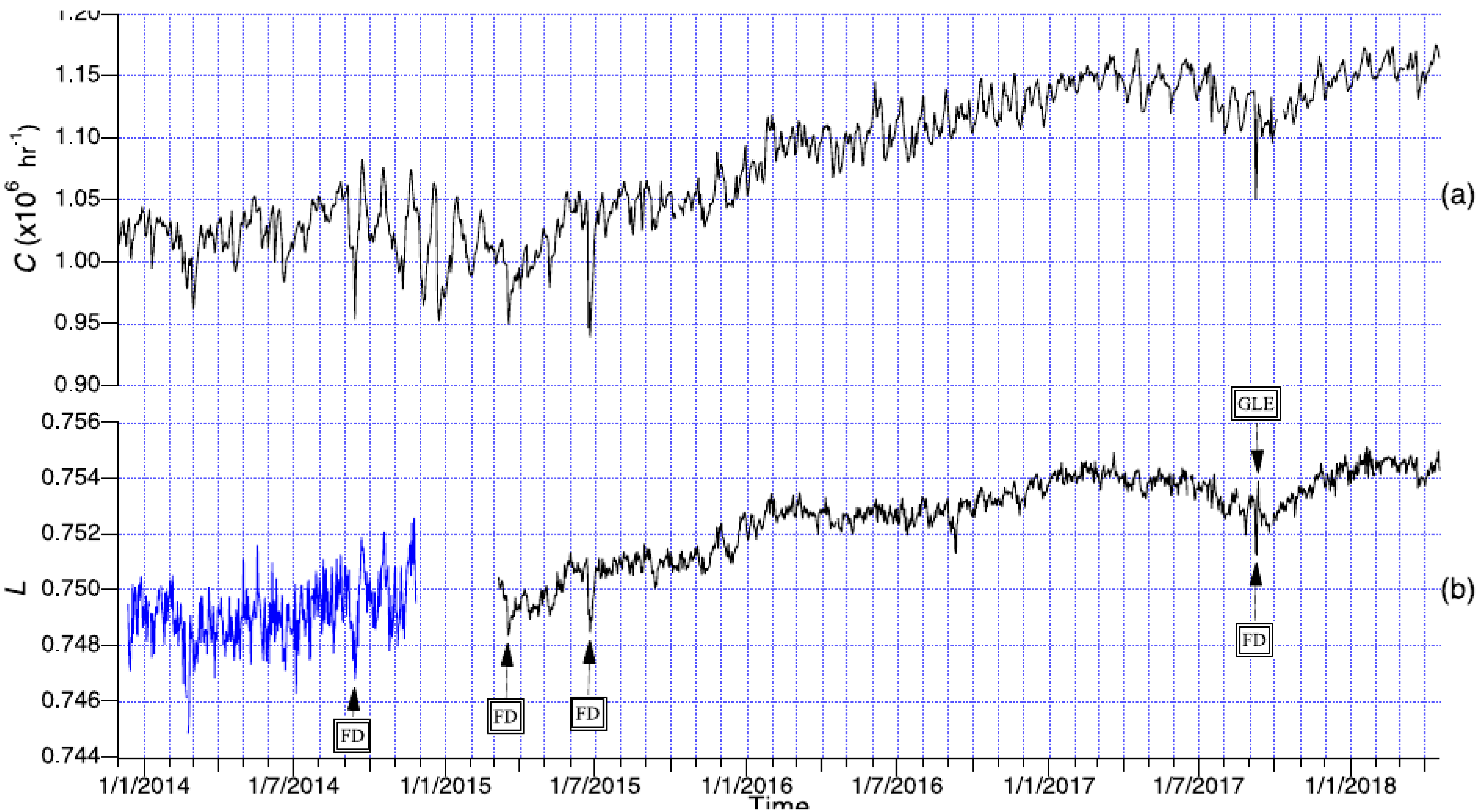

[C. Banglieng et al, 2020]

Leader fraction *L* and Count rate *C* at polar stations

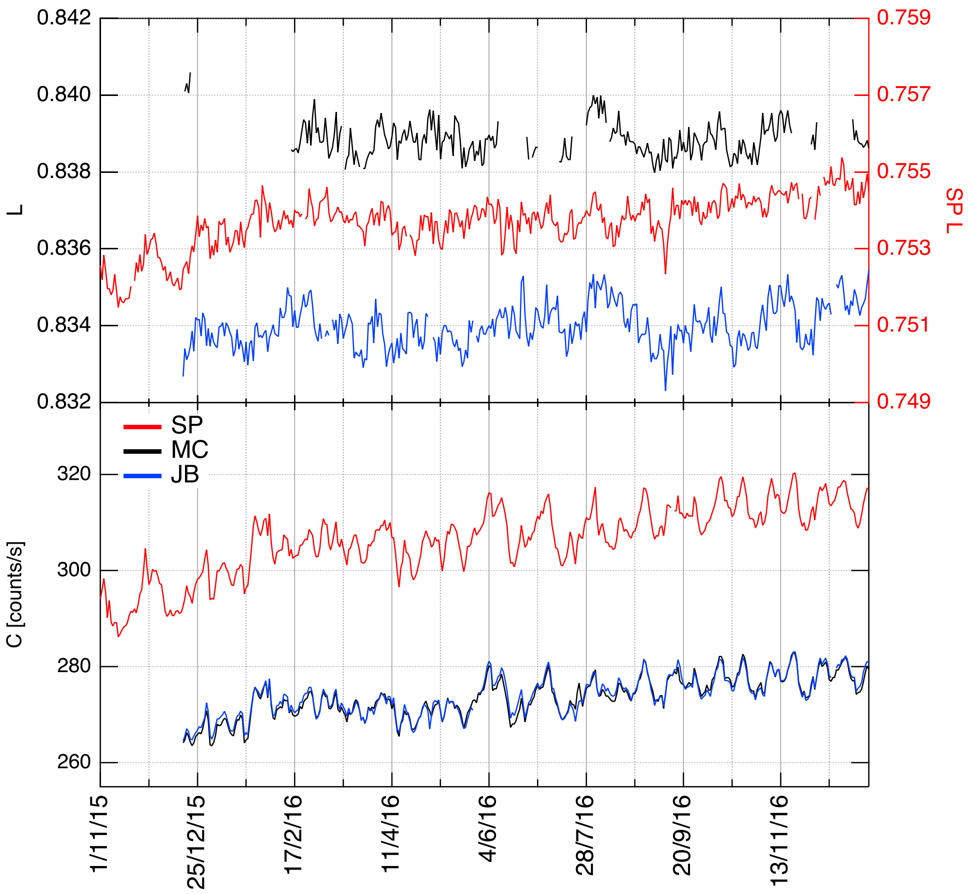

South Pole, McMurdo, Jang Bogo, ~2016

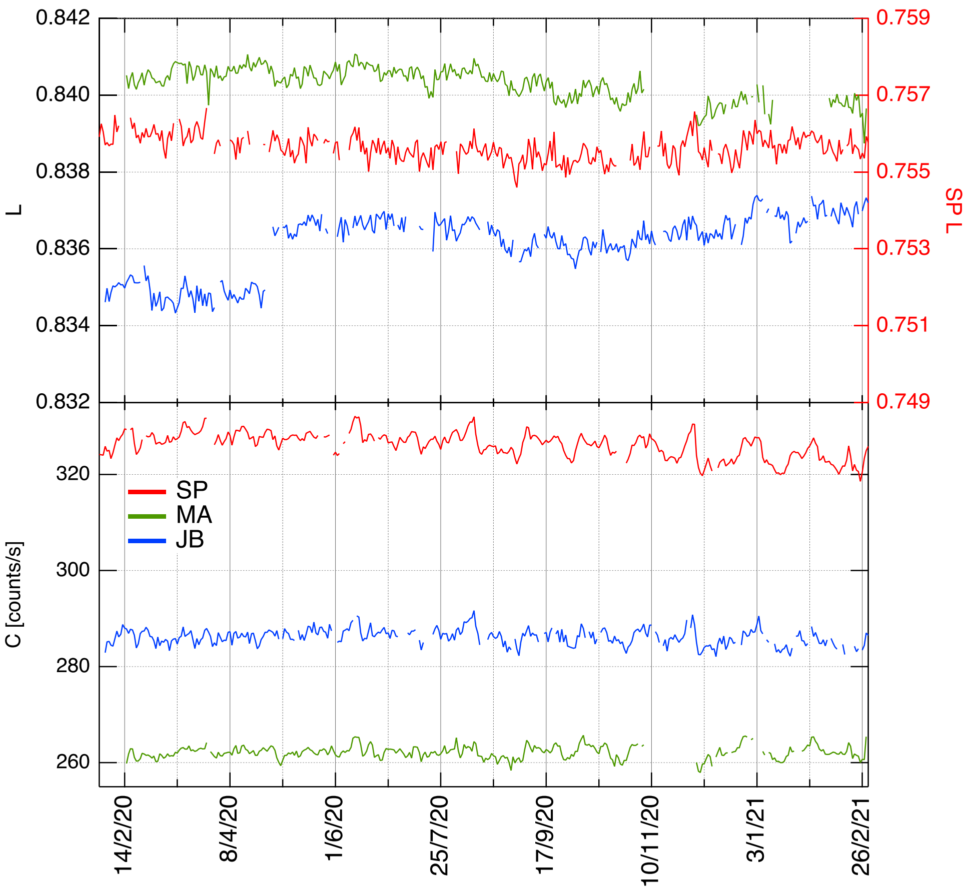

South Pole, Mawson, Jang Bogo, ~2020

[P. Muangha et al, in preparation]

SP *L* vs AMS-02 Spectral Index

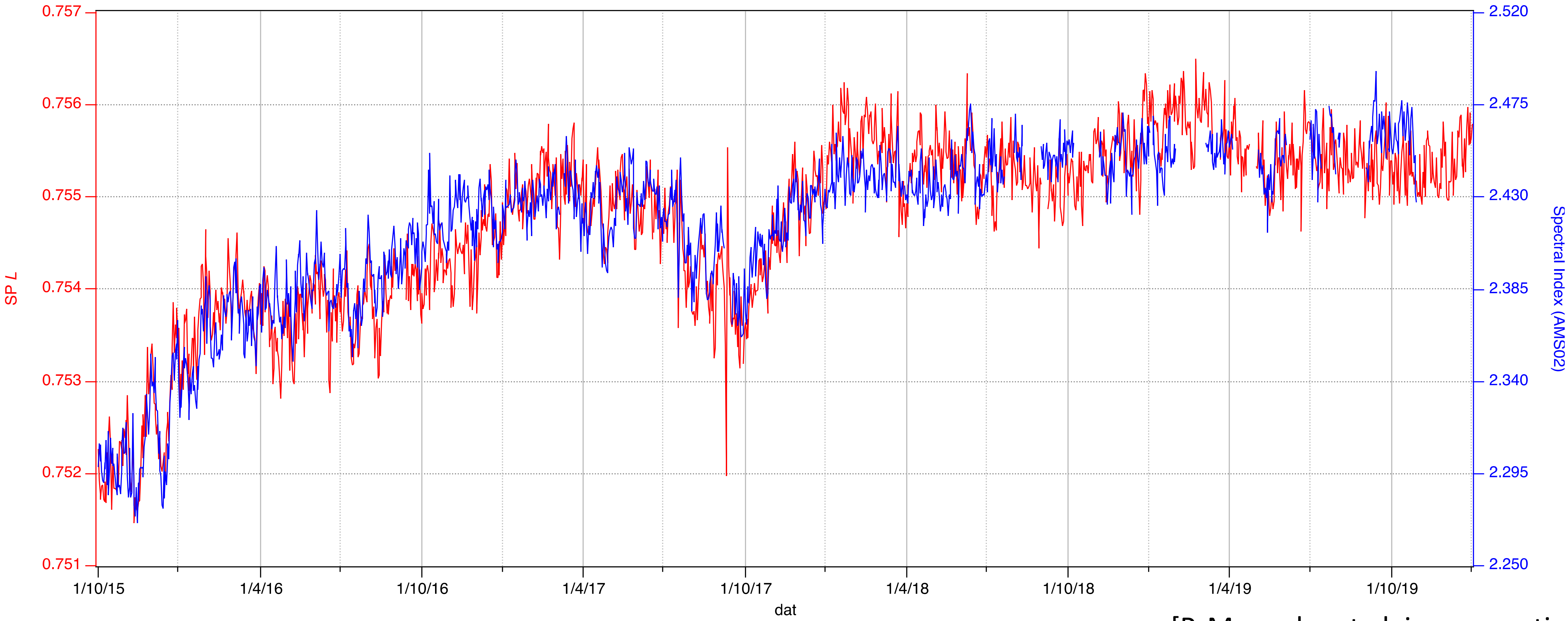

[P. Muangha et al, in preparation]

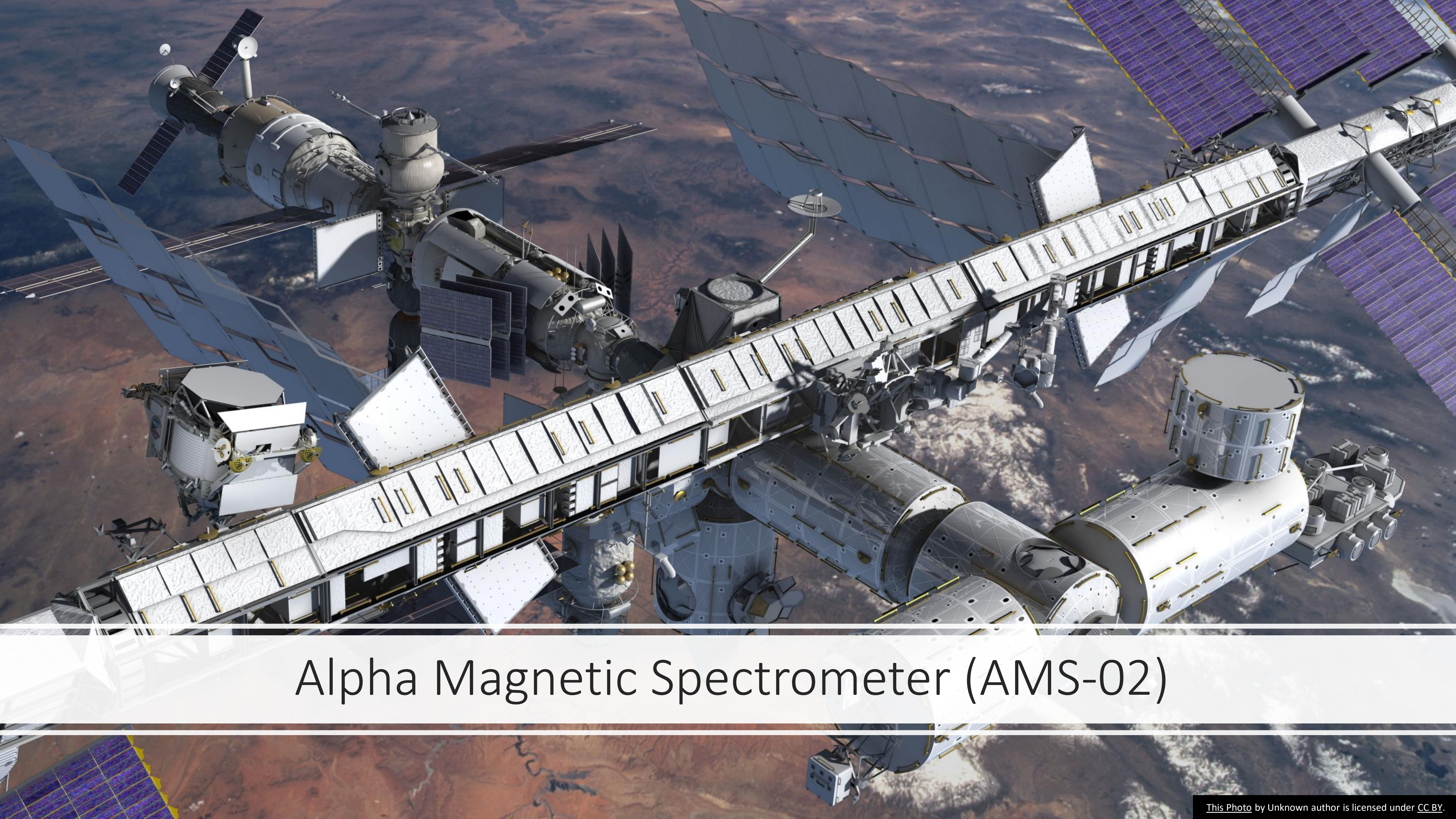

Alpha Magnetic Spectrometer (AMS-02)

Journal of Geophysical Research: Space Physics 10.1002/2016JA023515

Table 3. Proton Yield Functions of a Standard 3NM64 at Sea Level for Various Electronic Dead Times

R (GV)	E_k/Nucleon (GeV)	Counts Per Primary Flux (cm^2 sr) Dead Time 0 s	20 μs	100 μs	1.2 ms	4 ms
0.5	0.1249	—	—	—	—	—
0.7	0.2324	1.34e−2	1.33e−2	1.30e−2	1.19e−2	1.18e−2
1	0.4331	3.65e−1	3.62e−1	3.52e−1	3.20e−1	3.18e−1
2	1.271	1.12e+1	1.10e+1	1.07e+1	9.60e+0	9.51e+0
3	2.205	4.26e+1	4.21e+1	4.06e+1	3.61e+1	3.57e+1
5	4.149	1.61e+2	1.59e+2	1.52e+2	1.33e+2	1.31e+2
7	6.125	2.38e+2	2.34e+2	2.24e+2	1.94e+2	1.91e+2
10	9.106	3.78e+2	3.72e+2	3.54e+2	3.05e+2	3.01e+2
20	19.08	8.59e+2	8.43e+2	7.99e+2	6.81e+2	6.71e+2
30	29.08	1.31e+3	1.28e+3	1.21e+3	1.03e+3	1.01e+3
50	49.07	2.18e+3	2.14e+3	2.01e+3	1.70e+3	1.67e+3
70	69.07	3.04e+3	2.97e+3	2.79e+3	2.34e+3	2.30e+3
100	99.07	4.23e+3	4.13e+3	3.87e+3	3.24e+3	3.19e+3
200	199.1	8.06e+3	7.83e+3	7.30e+3	6.06e+3	5.95e+3
300	299.1	1.18e+4	1.14e+4	1.06e+4	8.76e+3	8.59e+3
500	499.1	1.86e+4	1.80e+4	1.67e+4	1.38e+4	1.35e+4
700	699.1	2.53e+4	2.44e+4	2.26e+4	1.85e+4	1.81e+4
1000	999.1	3.73e+4	3.58e+4			

P.-S. Mangeard et al. 2016b

Averaged AMS02 proton flux

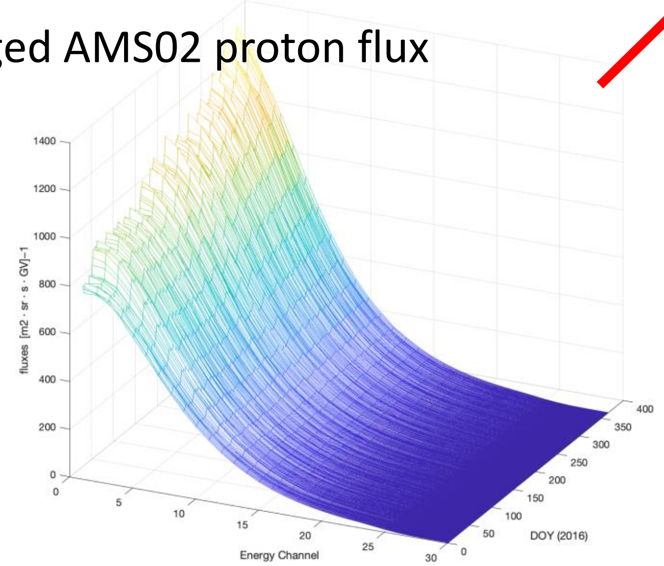

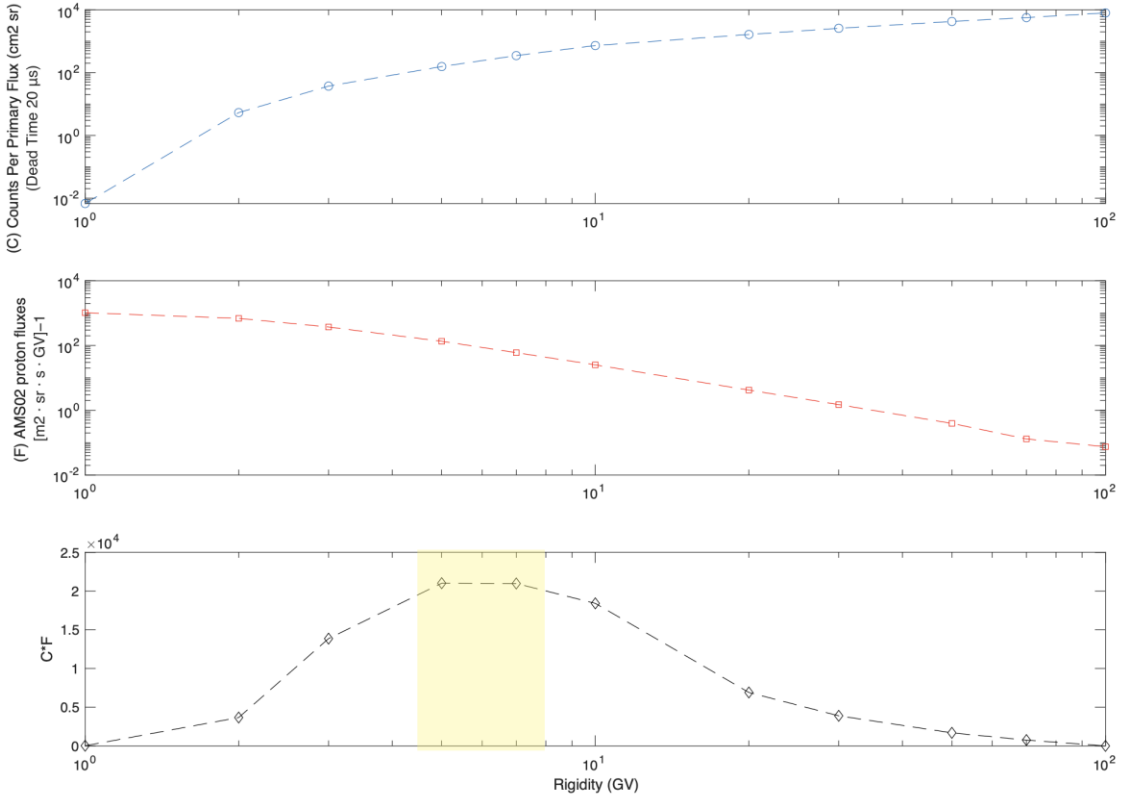

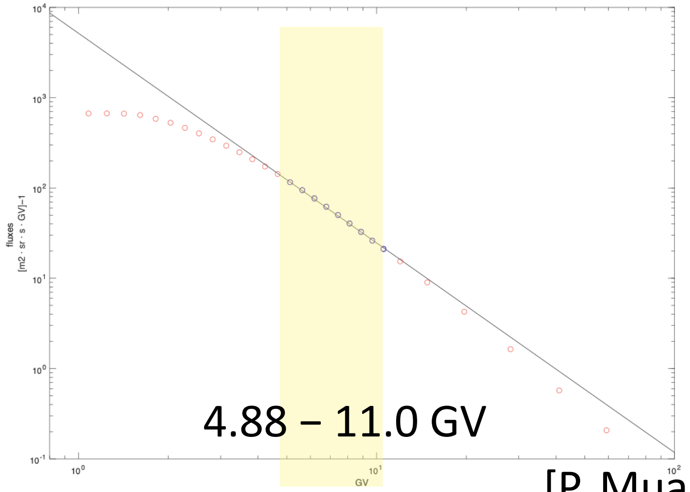

[P. Muangha et al, in preparation]

Jou

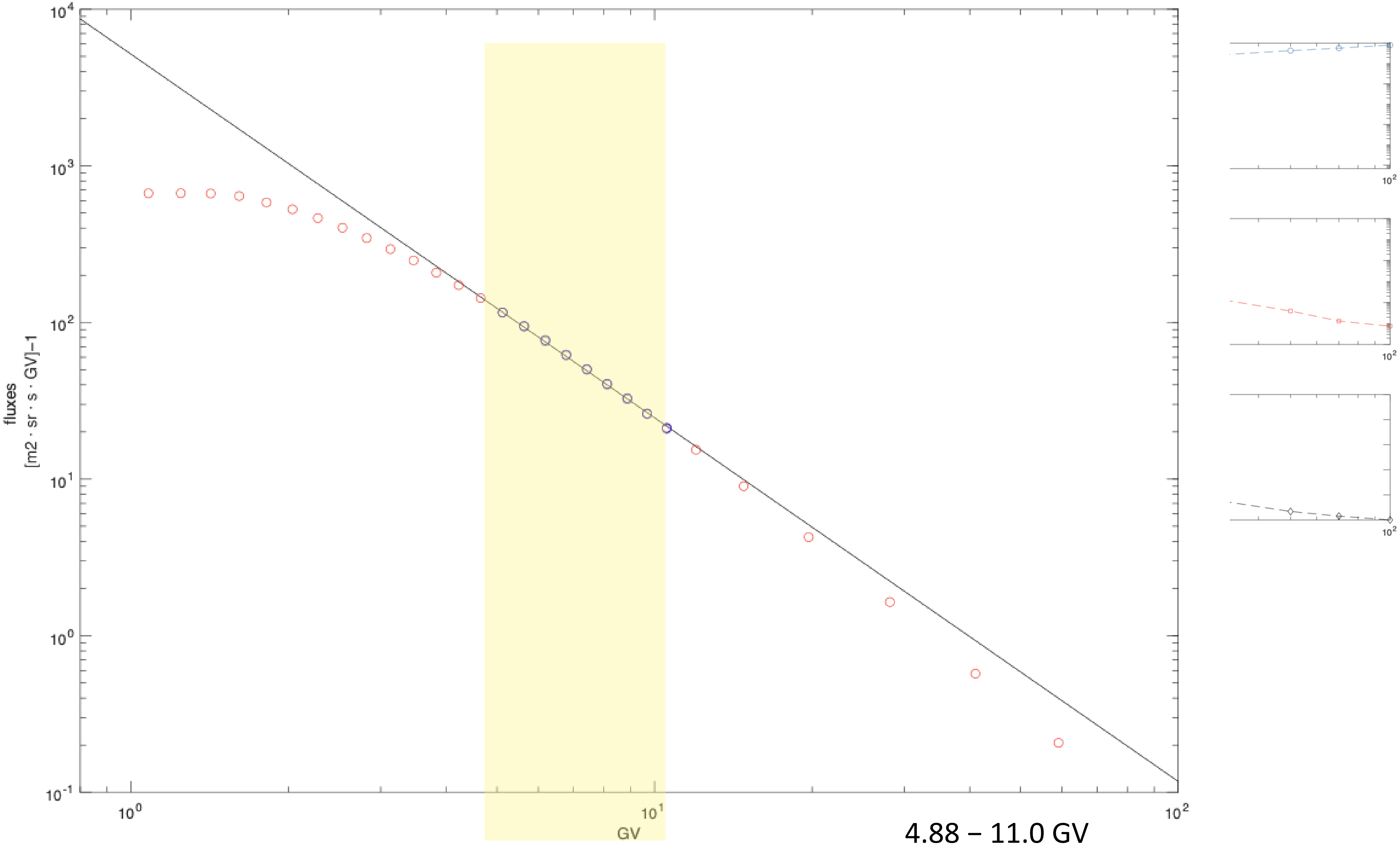

4.88 – 11.0 GV

[P. Muangha et al, in preparation]

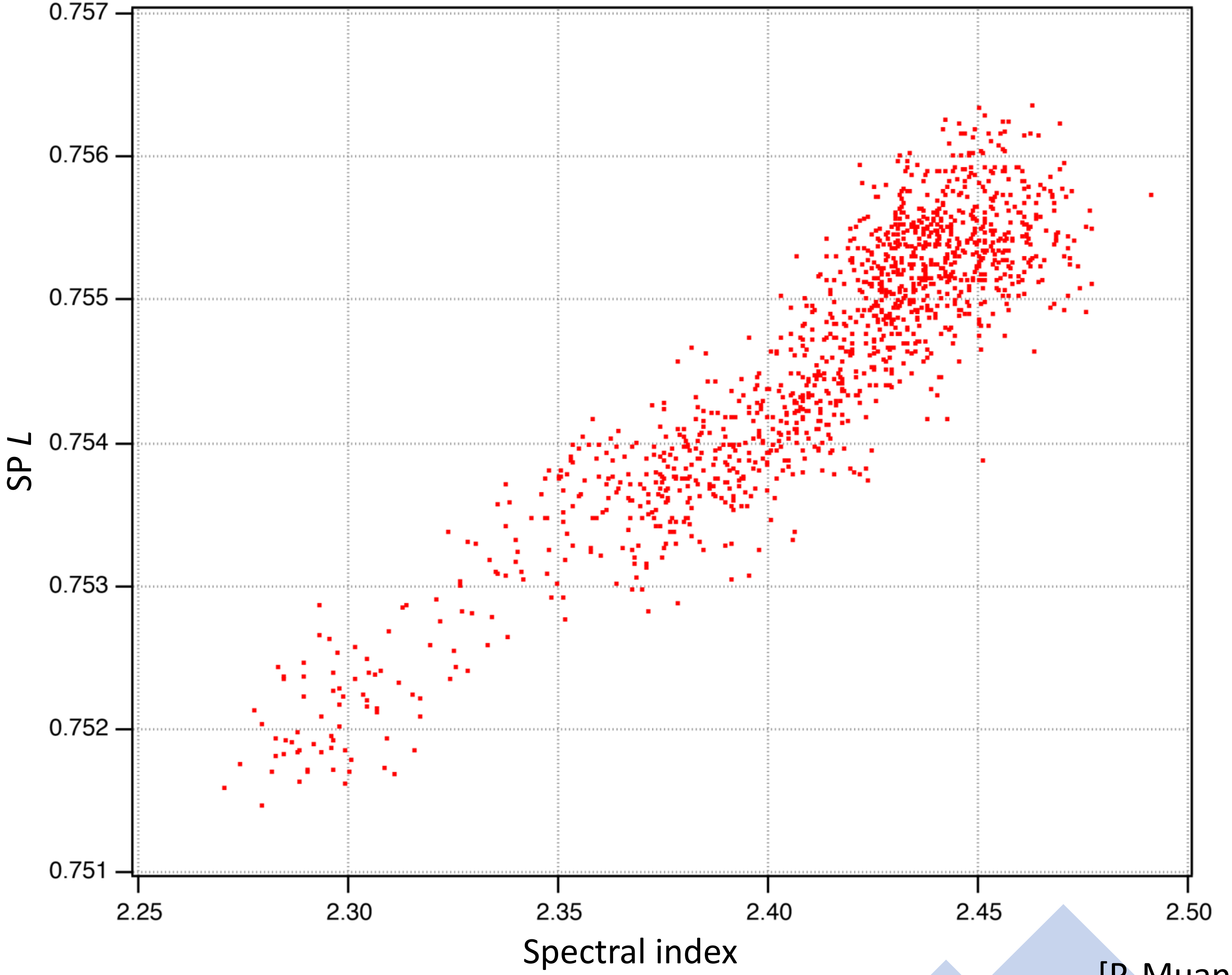

[P. Muangha et al, in preparation]

Leader fraction limitations

- The measured value of *L* is affected by high atmospheric humidity
- Analysis requires accumulating histograms: hourly data at best
- The value depends on the exact value of the dead time: not trivial to compare between stations

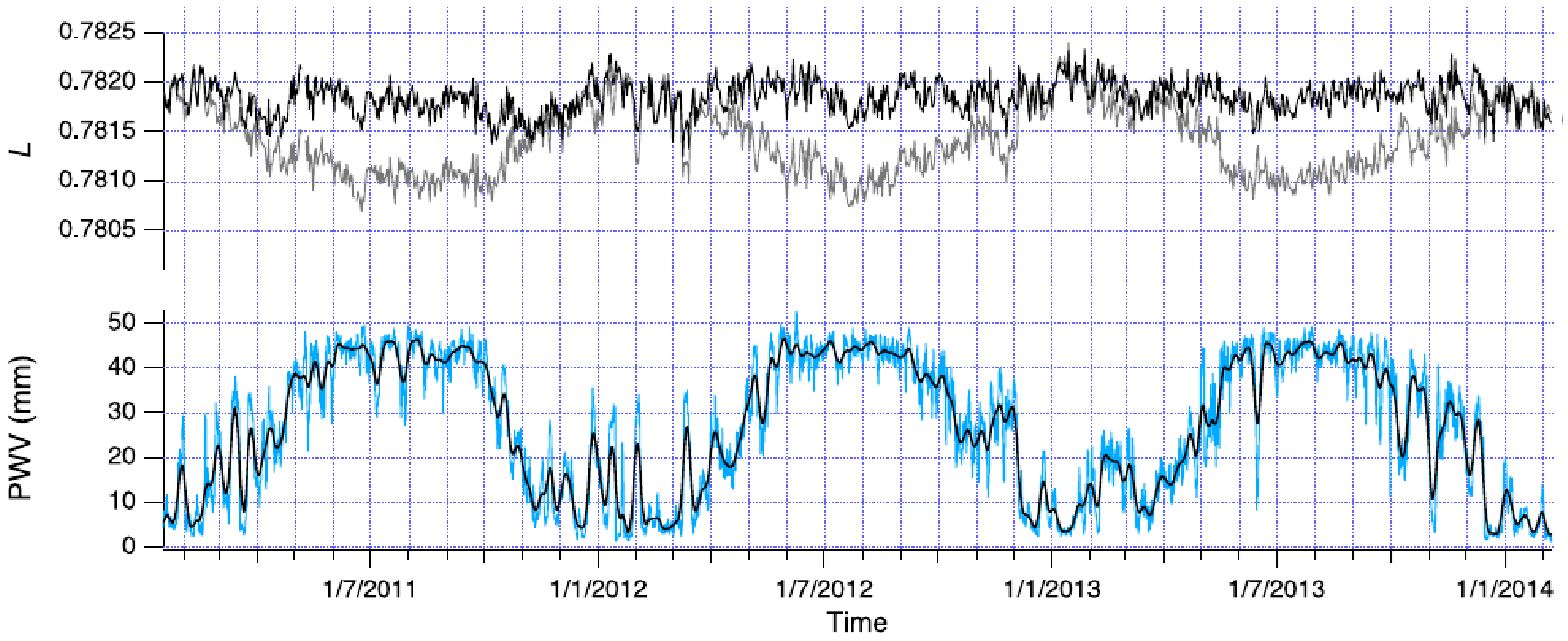

Cross-counter analysis

- *Synchronization of counter timer clocks allows to study correlations across the monitor*
- *Cross-L related to atmospheric cascades*

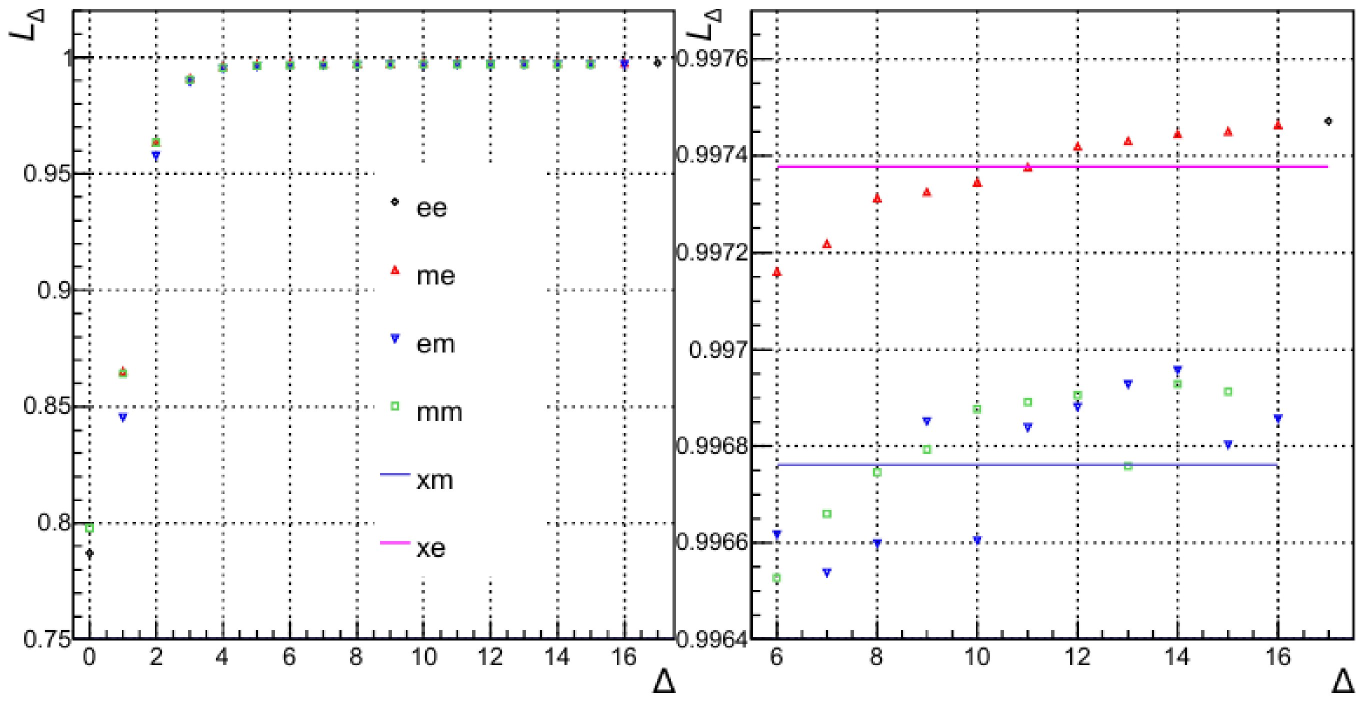

[A. Sáiz et al, 2019]

Princess Sirindhorn Neutron Monitor (PSNM)

- Doi Inthanon, Thailand (≈17 GV cutoff)
- Upgraded with cross-counter absolute timing for 18 counter tubes in horizontal row since 2015

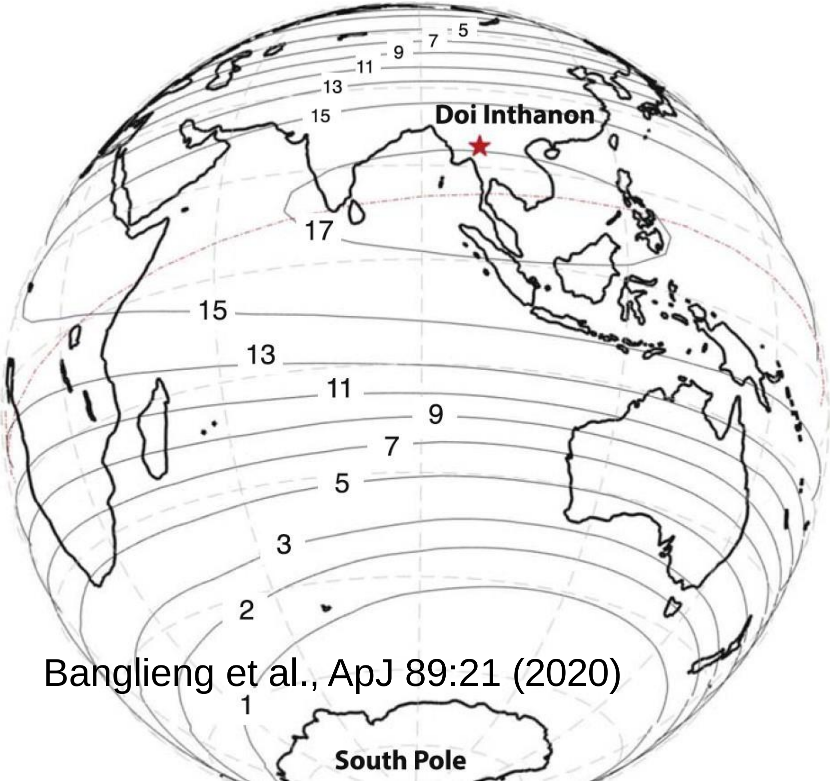

Banglieng et al., ApJ 89:21 (2020)

Effects from Positions of Counter Tubes

Leader fraction (L_{ij}) = fraction of counts on tube i which are not associated with a later count on tube j

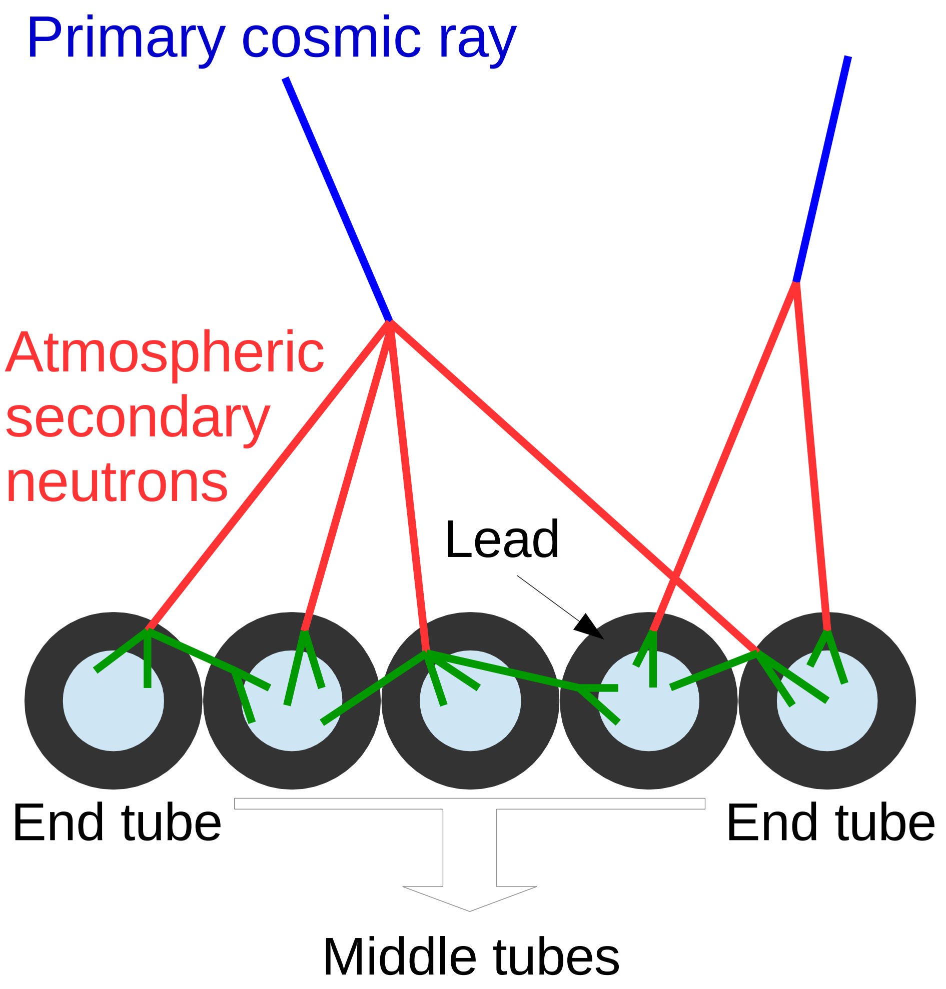

Associated counts between

- Near tubes (Δ ≤ 6): **same atmospheric secondaries** interacting with monitor
- Far tubes (Δ ≥ 12): shower from **same primary CR** (hinted by simulations, focus of this work)

- End tubes: less nearby lead, lower count rates
- Middle tubes: more nearby lead, higher chances for secondary interactions

ThaiSpacePhysics2022

LF vs Tube Separation

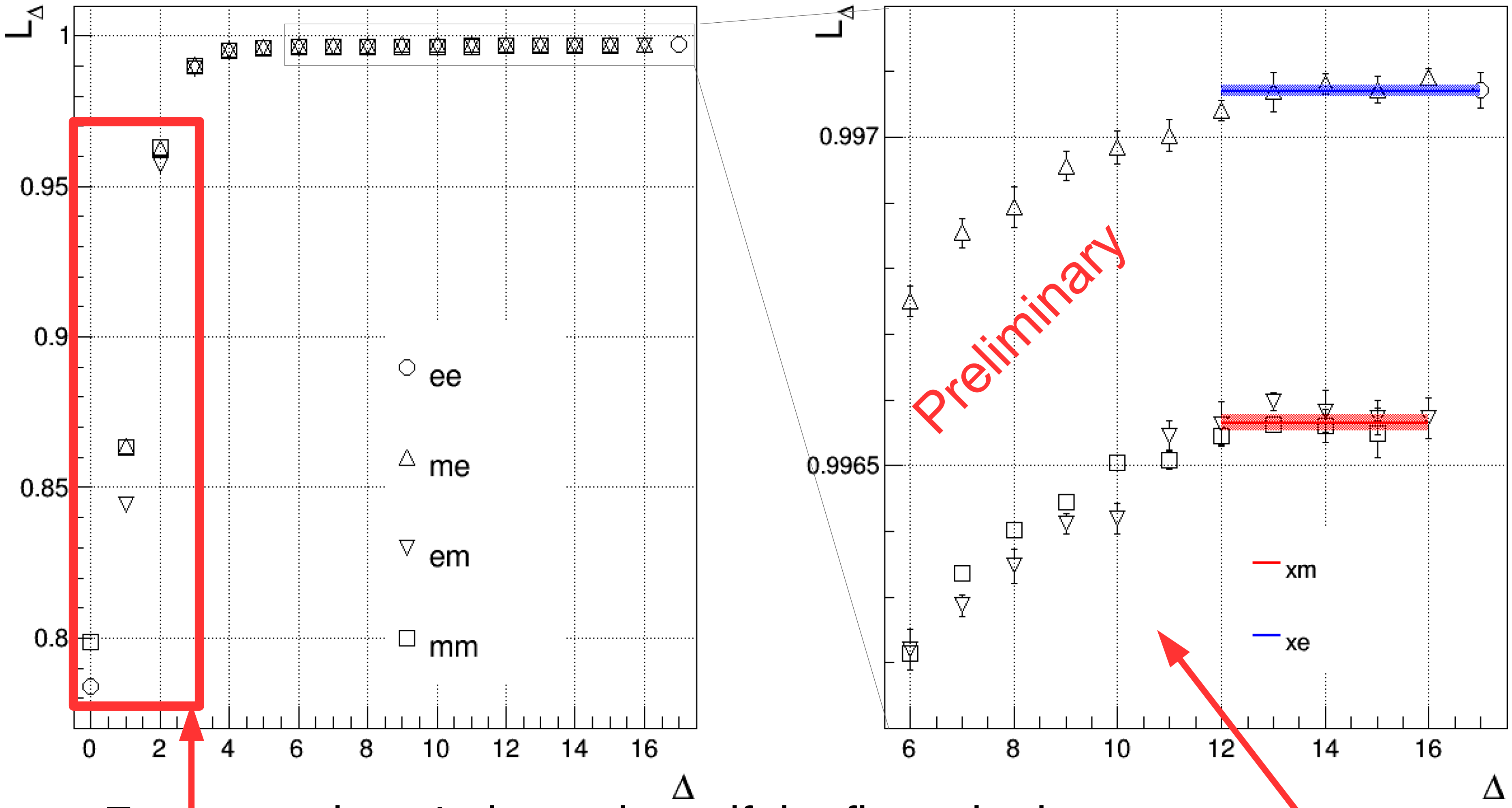

- For near tubes, L depends on if the first tube is m or e
- For far tube, L depends on if the later tube is m or e

Far-tube Leader Fraction Time Variation

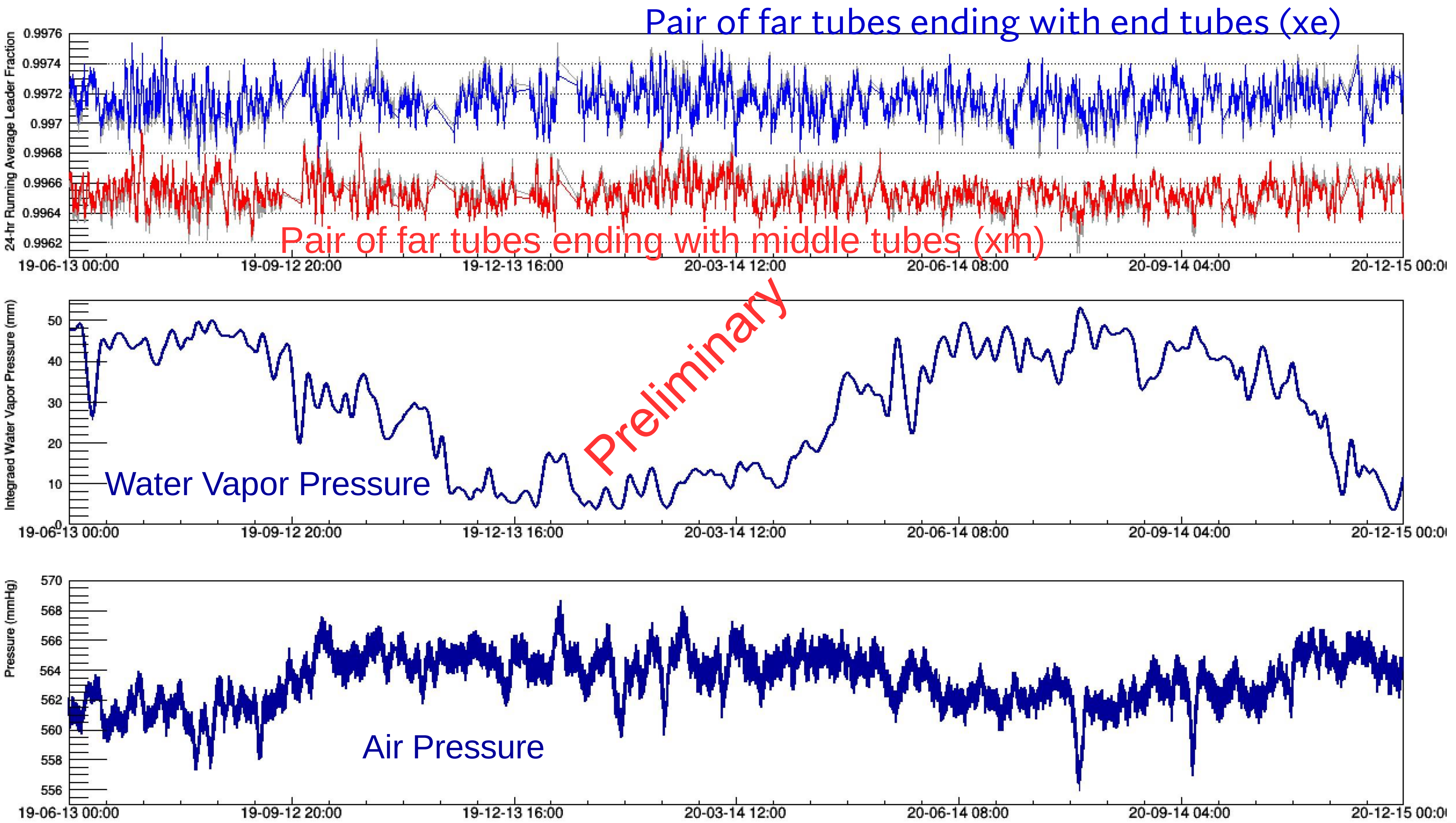

- L_{xm} and L_{xe} have been corrected for water vapor and air pressure
  - No time strong variation observed at PSNM
  - Normalization may relate to air-shower multiplicity

Cross-counter leader fraction for different counter combinations at Mawson

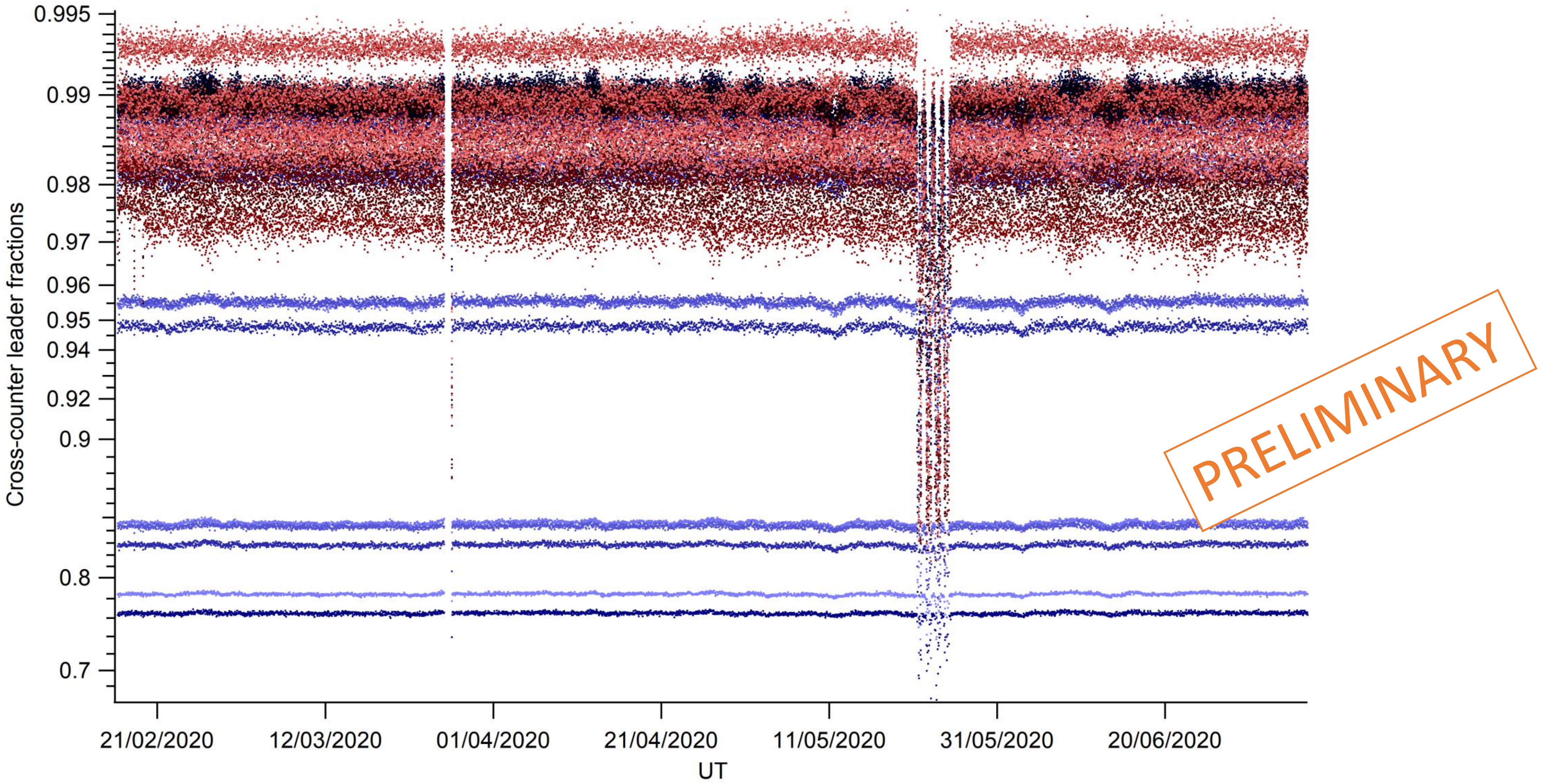

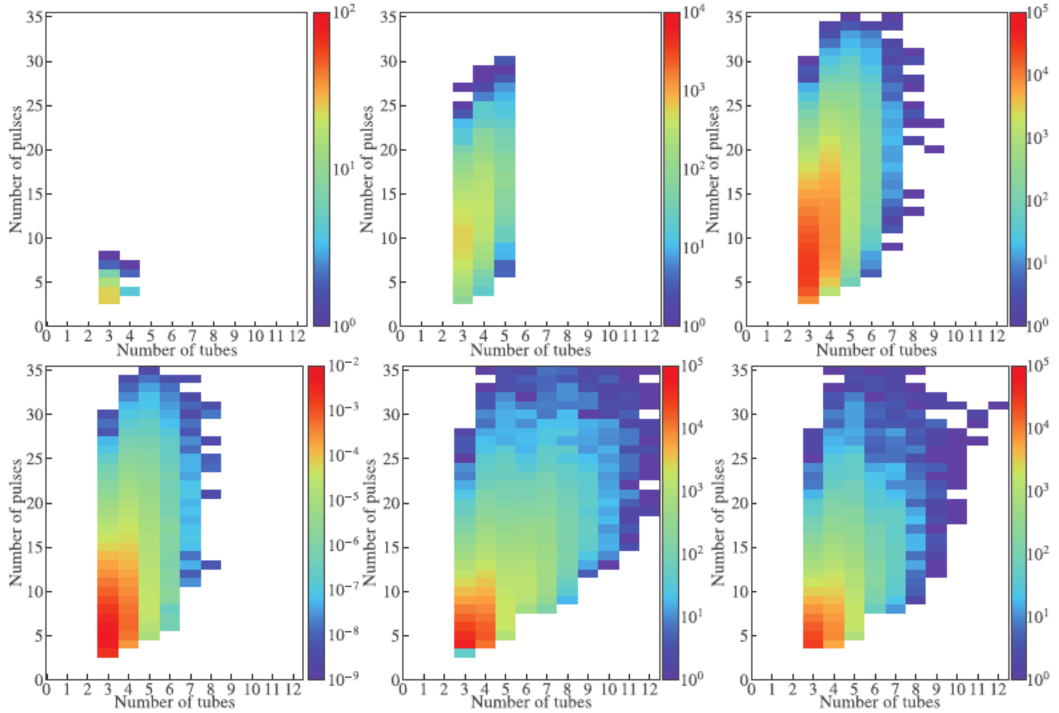

Comprehensive analysis

Individual "cluster" events can be sampled and analyzed in detail

[P. Evenson et al, 2021]

PSNM Interaction Histories

Actual air shower core (left) and two simulated 100 GeV neutrons. Time runs upward; blue lines are one millisecond apart.

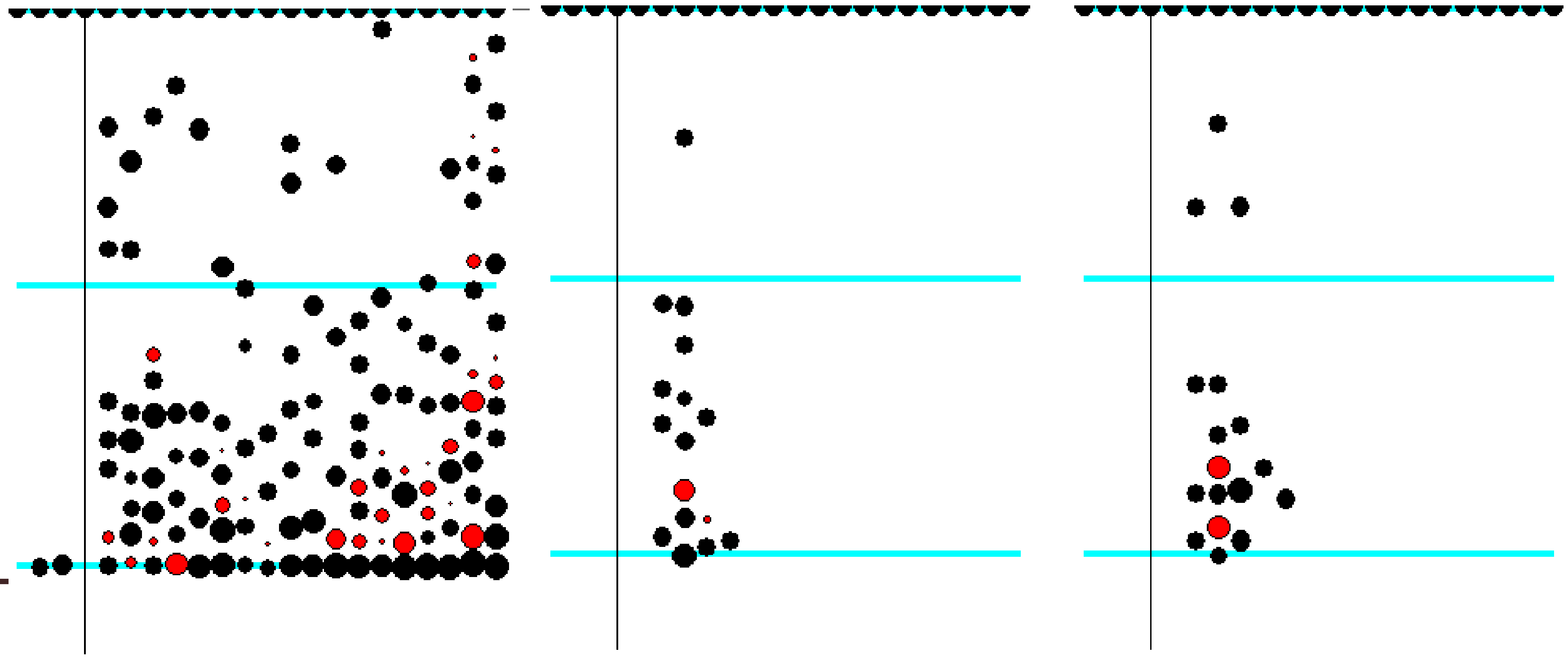

PSNM Simulations

In each case the number of detectors hit is plotted horizontally, while the total number of hits is plotted vertically.

Left: 1 GeV neutron pencil beam.

Center: 100 GeV neutron pencil beam.

Right: 1 to 100 GeV, E^{-1} spectrum distributed in location and incident direction.

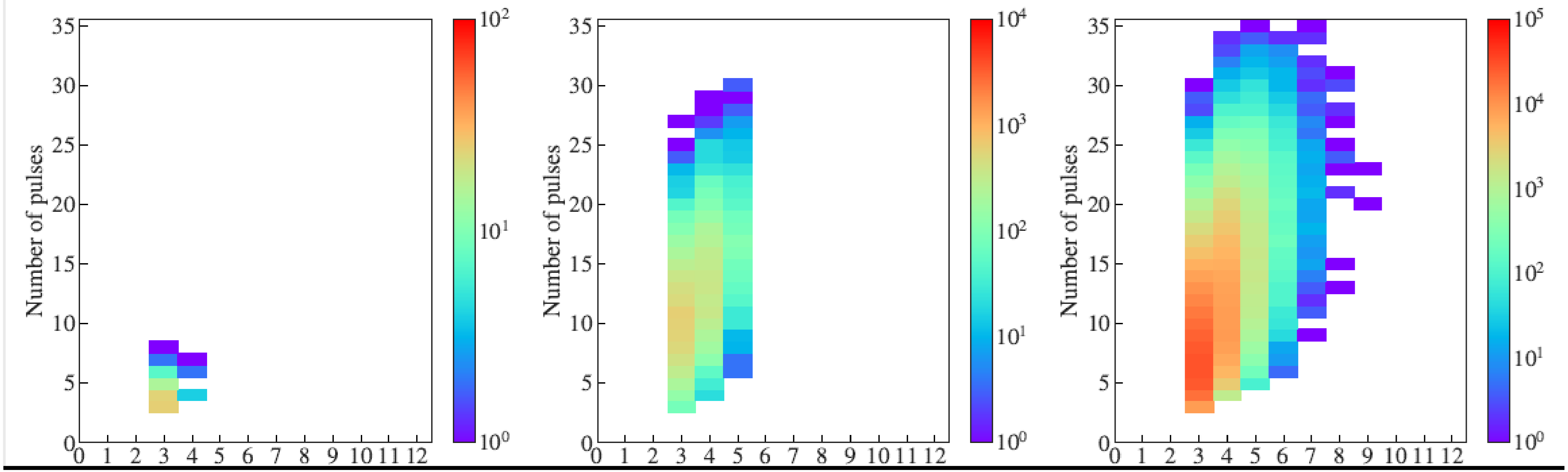

PSNM Simulation and Data

Left: Simulation re-weighted to $E^{-2.5}$.

Center: Two days of actual data.

Right: Data selected for a single, contiguous span of hit detectors with no hits in the end detectors.

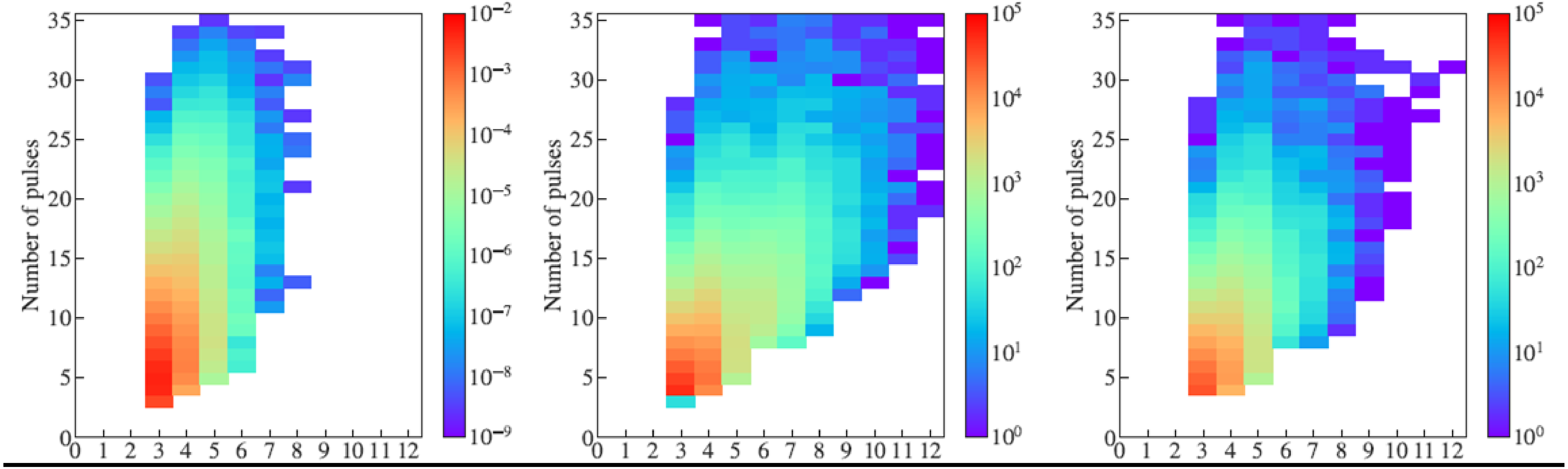

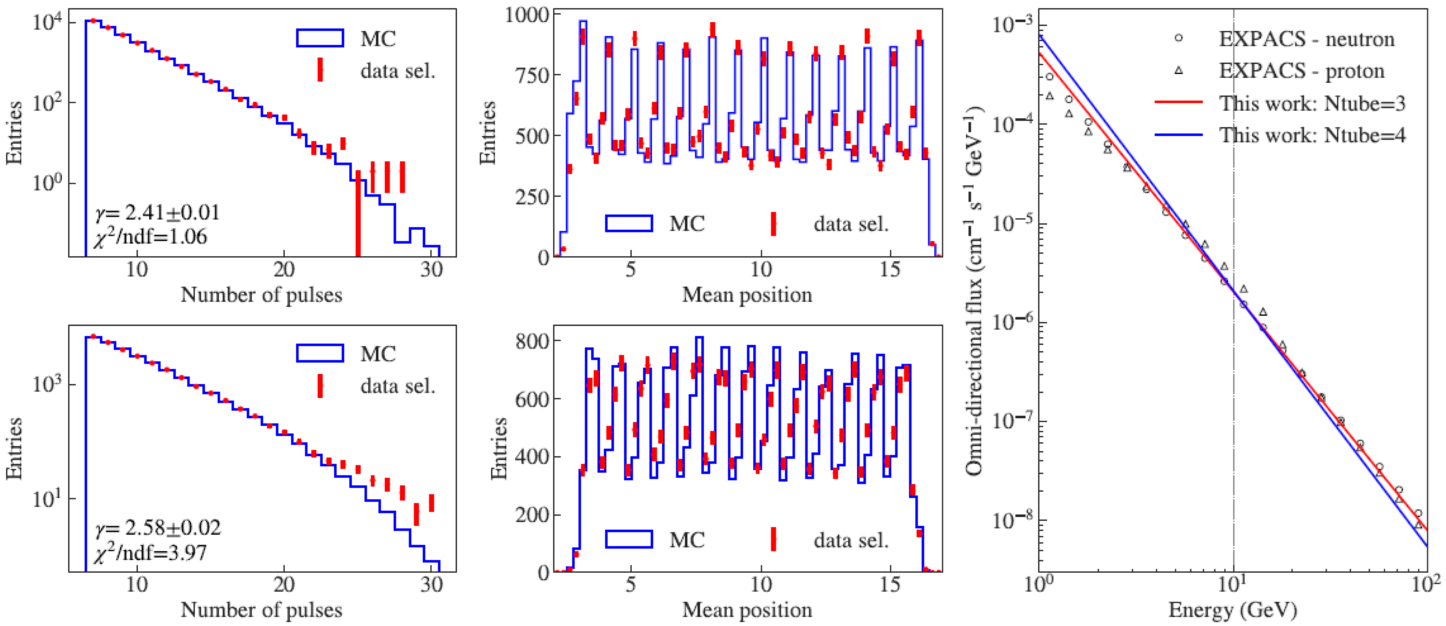

Final Analysis Presented at the ICRC in 2021

From PoS(ICRC2021)1240

Further progress has been presented at meetings, but this is currently the latest printed version.

Multiplicity studies in the near future

- Connection between CR spectrum and other multiplicity data?
- Monte Carlo simulations still not perfect
- Modern electronic components can be a game changer
- Artificial intelligence may help, but probably not in the near future
- New theoretical approaches?

Thank you